

578630  
P. 81



**NASA/USRA UNIVERSITY  
ADVANCED DESIGN PROGRAM  
1989-1990**

**UNIVERSITY SPONSOR  
BOEING COMMERCIAL AIRPLANE COMPANY**

**FINAL DESIGN PROPOSAL**

**DAWDLER**

**A Proposal in Response to a Low Reynolds Number  
Station Keeping Mission**

**May 1990**

**Department of Aerospace and Mechanical Engineering  
University of Notre Dame  
Notre Dame, IN 46556**

**(NASA-CR-186668) PROJECT DAWDLER: A  
PROPOSAL IN RESPONSE TO A LOW REYNOLDS  
NUMBER STATION KEEPING MISSION Final Design  
Proposal (Notre Dame Univ.) 81 p CSCL 01C**

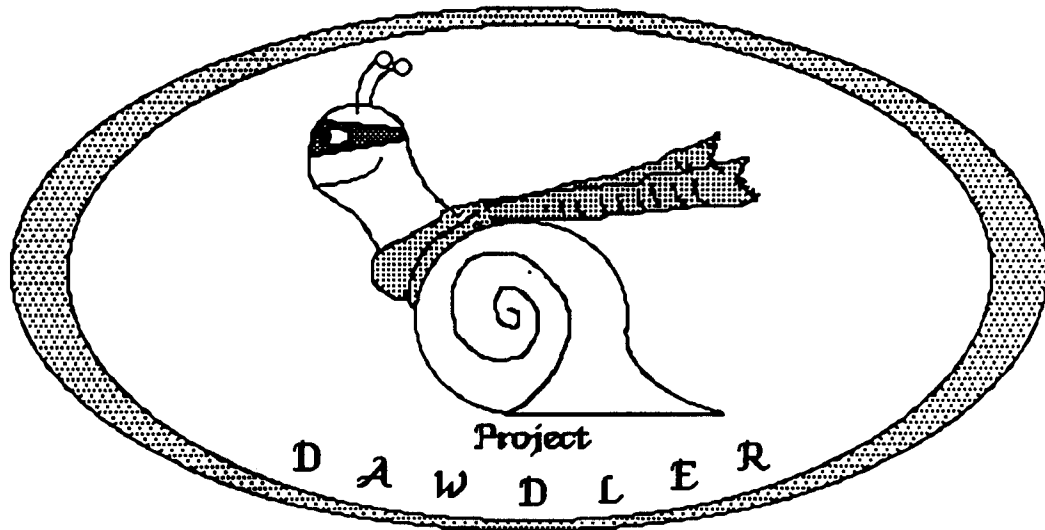
**N90-25128**

**Unclass**

**63/05 0289187**

# *Project Dawdler*

*— design proposal for a remotely piloted low Reynolds number aircraft —*



Submitted by Squad E in response to Aerospace Design Request for Proposals

Squad E members:

Rich Bartilotti  
Jill Coakley  
Warren Golla

Glenn Scamman  
Hòa T. Trần  
Chris Trippel

The Design Squad ...

The Dawdler

Design Proposal for

A Remotely Piloted Low Reynolds Number Aircraft

Submitted 07 May 1990 in response to "Aerospace Design - Request for Proposals"  
University of Notre Dame Department of Aerospace and Mechanical Engineering

1990 Design Squad E members:

Rich Bartilotti	Aerodynamics
Jill Coakley	Stability and Control
Warren Golla	Take-off Performance, Tech Demo
Glenn Scamman	Propulsion, Performance, Tech Demo
Hòa T. Trần	Squad Leader
Chris Trippel	Weights and Structures, Tech Demo

This document is set in Times Roman.

# Table of Contents

	Page
<b>Executive Summary</b> .....	iii
<b>Three-View Drawing of The Dawdler</b> .....	v
<b>Specifications Summary</b> .....	vi
<b>I Mission Study</b> .....	1
<b>II Concept Selection Studies</b> .....	6
<b>III Aerodynamic Design</b> .....	9
3.1 Wing Selection .....	9
3.2 Airfoil Selection for the Wing .....	10
3.3 Canard Sizing.....	11
3.4 Aircraft Aerodynamics.....	12
<b>IV Propulsion System</b> .....	15
4.1 System Selection .....	15
4.2 System Integration .....	16
4.3 Motor Sizing.....	17
4.4 Propeller Design.....	19
4.5 Propulsion System Performance Predictions .....	21
4.6 Engine Control .....	24
<b>V Weight Estimation</b> .....	27
5.1 Weight Percentages .....	27
5.2 Center of Gravity Estimation .....	28
<b>VI Stability &amp; Control</b> .....	31
6.1 Lateral and Directional.....	31
6.2 Wing Dihedral .....	31
6.3 Vertical Tail Sizing.....	31
6.4 Stability Derivatives.....	32
6.5 Rudder Deflection.....	34
6.6 Longitudinal Stability.....	35

<b>VII Performance Estimation</b> .....	36
7.1 Take-off Performance .....	36
7.2 Range and Endurance.....	42
7.3 Power Required and Available .....	42
7.4 Climbing and Gliding Performance.....	43
<b>VIII Structural Design</b> .....	45
8.1 Flight and Ground Load Estimation .....	45
8.2 Structural Components .....	46
8.3 Material Selection .....	49
<b>IX Technology Demonstrator</b> .....	50
9.1 Configurational Data and Geometry .....	50
9.1.1 Airplane.....	50
9.1.2 Launch Cart.....	52
9.2 Weights.....	52
9.3 Manufacturing and Cost Details .....	53
9.4 Test Safety Considerations.....	56
9.5 Test Results.....	56
9.5.1 Launch Cart.....	56
9.5.2 Aircraft.....	57
9.6 Recommendations.....	59
<b>X Extension of Mission to High Altitude Long Duration Station Keeping Mission</b> .....	61
<b>References</b> .....	63
<b>Appendix A: Stability Derivative Estimates</b> .....	64
A.1 Lateral .....	65
A.2 Directional.....	65
<b>Appendix B: Zoom Take-off Analysis</b> .....	66
B.1 Mathematical Basis for Numerical Solution.....	67
B.2 Assumptions and Particular Design Values Used .....	68
B.3 Zoom Take-off Computer Analysis Code.....	70
B.4 Validation of Numerical (Computer-Derived) Results.....	72

# Executive Summary

In direct response to "Request for Proposals: FLIGHT AT VERY LOW REYNOLDS NUMBERS - A STATION KEEPING MISSION," the members of Design Squad E present Project Dawdler: a remotely-piloted airplane supported by an independently controlled take-off cart. The following gives a brief introduction to Project Dawdler's overall mission and design, and is followed by a three-view drawing of the Dawdler and a specifications summary.

The Dawdler is a remotely-piloted airplane designed to fly in an environmentally-controlled closed course (300 ft x 120 ft x 25 ft) at a Reynolds number of  $10^5$  (based on mean wing chord) and at a cruise velocity of 25 ft/s. It will be able to take-off and climb to a cruise altitude of 20 ft within a distance of 150 ft, at which point it will have just enough stored power to fly a "figure-eight" course three times and land within the same take-off/landing strip from which it took off (150 ft x 30 ft).

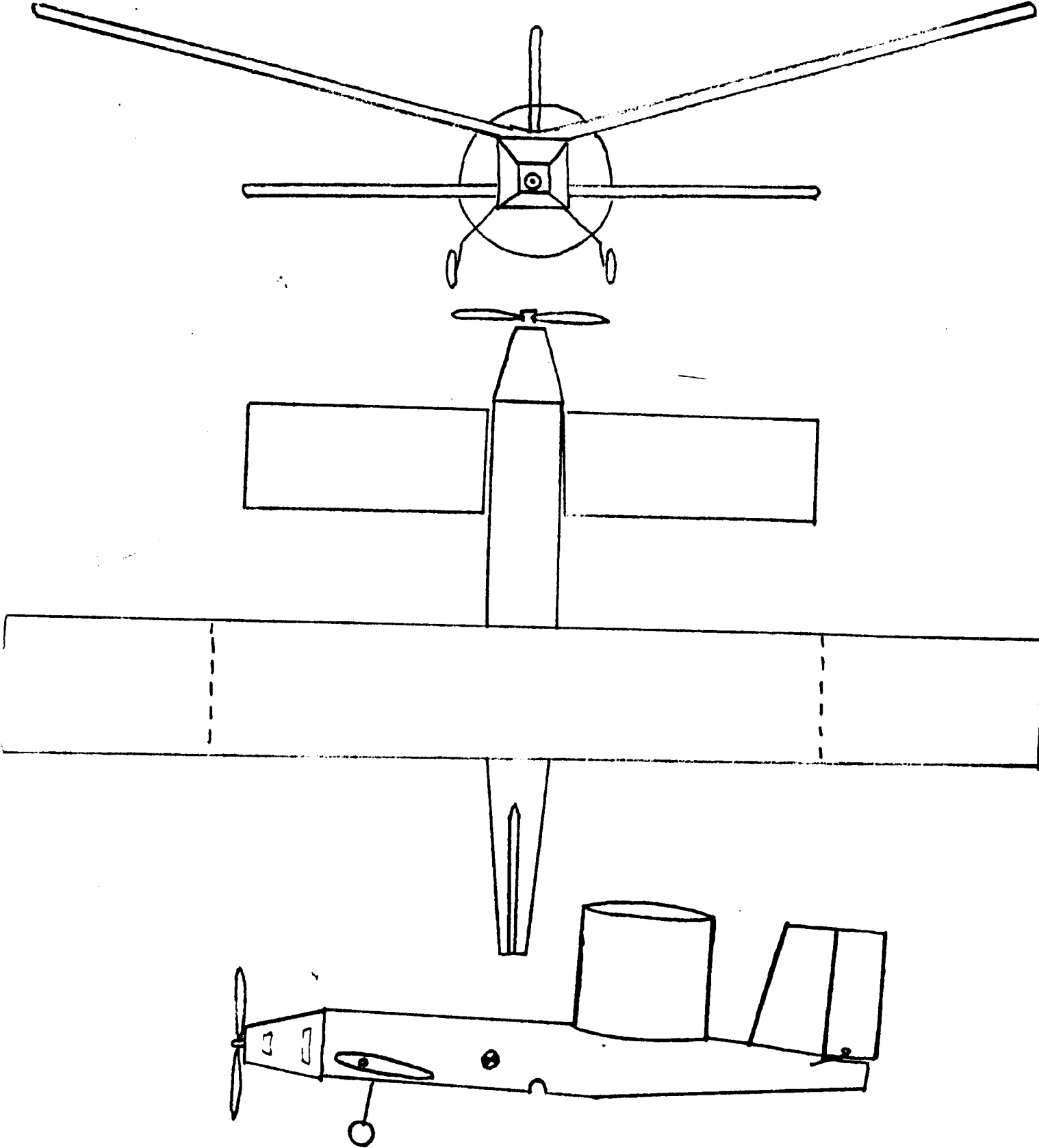
The two primary goals of this study were to minimize the flight Reynolds number and to maximize the loiter time. With this in mind, the general design of the airplane was guided by the belief that a relatively light aircraft producing a fairly large amount of lift would be the best approach. For this reason the Dawdler utilizes a canard rather than a conventional tail for longitudinal control, primarily because the canard contributes a positive lift component. Due to the relative size of the canard (it produces 30% of the total lift), the Dawdler, with its low-mounted canard and high-mounted wing, actually resembles a tandem wing aircraft. Furthermore, the canard is fully movable in order to provide the necessary pitch control. The Dawdler also has a single vertical tail mounted behind the wing for lateral stability, half of which is used as a rudder for yaw control. Because ailerons were excluded from the design due to the added weight associated with their inclusion, a  $13^\circ$  dihedral angle was incorporated into the design of the wing in order to provide the proper rolling ability necessary to turn the plane.

Due to the fact that the power required to take-off and climb to altitude is much greater than that required for cruise flight and simple turning maneuvers, it was decided that a take-off cart be used. This allowed for the use of a smaller sized electric motor (Astro 035) and a corresponding reduction in the amount of battery storage needed, all of which contributed to a lighter design. The cart itself is designed to accelerate the plane to a take-off speed of approximately 35 ft/s, which should give the aircraft sufficient kinetic energy to zoom to cruise altitude.

Based on the current design, there are two unknowns which could possibly threaten the success of Project Dawdler. First, how will the fully-movable canard with its large appropriation of total lift affect the performance of the plane, and secondly, will the take-off procedure go as according to plans? These are questions which can only be answered by a prototype. We do feel that Project Dawdler is a solid design, and with continued support and development, it will ultimately prove to be a success.

- Design Squad E

# Three-View Drawing of The Dawdler





## Specifications Summary

<b>Fuselage:</b>	length	37 in
	max diameter	3.5 in
	average diameter	3.25 in
	fineness ratio	10.57
	payload volume	190 in <sup>3</sup>
<b>Wing:</b>	aspect ratio	7.72
	span	60 in
	root chord	7.8 in
	taper ratio	1.0
	dihedral	13°
	airfoil section	Clark-Y
	incidence angle	4.35°
<b>Canard:</b>	area	201.6 in <sup>2</sup>
	aspect ratio	5.55
	root chord	6.0 in
	taper ratio	1.0
	incidence angle	5.85°
	airfoil section	Clark-Y
<b>Vertical Tail:</b>	area	49.5 in <sup>2</sup>
	aspect ratio	1.64
	root chord	5.5 in
	taper ratio	1.0
	airfoil section	flat plate
<b>Propulsion:</b>	motor	Astro 035
	placement	front
	propeller	9-6
	number of blades	2
<b>Weights:</b>	total	37.1 oz
	engine	6.9 oz
	avionics	4.3 oz
<b>Performance:</b>	Vmin	21 ft/s
	Vmax	40 ft/s
	Vstall	21 ft/s
	range	1760 yd
	endurance	193 s

# I

## Mission Study

The following is an exact transcript of the original Request for Proposals:

UNIVERSITY OF NOTRE DAME  
DEPARTMENT OF AEROSPACE AND MECHANICAL ENGINEERING

AE441: Aerospace Design: Request for Proposals

Spring 1990

### FLIGHT AT VERY LOW REYNOLDS NUMBERS - A STATION KEEPING MISSION

#### OPPORTUNITY

Most conventional flight vehicles are designed to operate in a flight regime such that the Reynolds number based on mean wing chord is in excess of  $10^6$  and some currently are approaching  $10^8$ . Recently there has been interest expressed in vehicles which would operate at much lower Reynolds numbers, less than  $10^5$ . Particular applications are low speed flight at very high altitudes, low altitude flight of very small aircraft and flight in other planets' atmospheres such as Mars. There are many unique problems associated with low speed flight which pose challenges to the aircraft designer and which must be addressed in order to understand how to exploit this low Reynolds number flight regime. Since many of the anticipated missions for this type of aircraft are unmanned, it is necessary to couple developments in unmanned aircraft development with our knowledge of low Reynolds number aerodynamics in order to develop an aircraft which can fly as slow as possible at sea level conditions. This study will help to better understand the problems associated with flight at these very low Reynolds numbers. Considering the potential applications, the aircraft must also be very robust in its control and be highly durable.

#### OBJECTIVES

1. Develop a proposal for an aircraft and associated flight control system which must be able to:
  - a. Maintain level controlled flight and fly a closed course at flight speeds corresponding to Reynolds numbers less than  $2 \times 10^5$  and as close to  $1 \times 10^5$  as possible. The greatest measure of merit is associated with achieving the lowest

- mean chord Reynolds number possible and maximizing the loiter time on a closed course.
- b. Be maneuverable and controllable so that it can fly a closed pattern and remain within a limited airspace.
  - c. Use a propulsion system which is non-airbreathing and does not emit any mass, (i.e. rocket, etc.).
  - d. Be able to be remotely controlled by a pilot with minimal flying experience or an autonomous onboard control system.
  - e. Carry an instrument package payload which weighs 2.0 oz and is 2" x 2" x 2" in size.
2. Take full advantage of the latest technologies associated with lightweight, low cost radio controlled aircraft and unconventional propulsion systems.
  3. All possible considerations must be taken to avoid damage to surroundings or personal injury in case of system malfunction.
  4. Develop a flying prototype for the system defined above. The prototype must be capable of demonstrating the flight worthiness of the basic vehicle and flight control system. The prototype will be required to fly a closed figure "8" course within a highly constrained envelope. A basic test program for the prototype must be developed and demonstrated with flight tests.
  5. Evaluate the feasibility of the extension of the aircraft developed under this project to high altitude station keeping application for atmospheric sampling.

#### **SYSTEM REQUIREMENTS AND CONSTRAINTS**

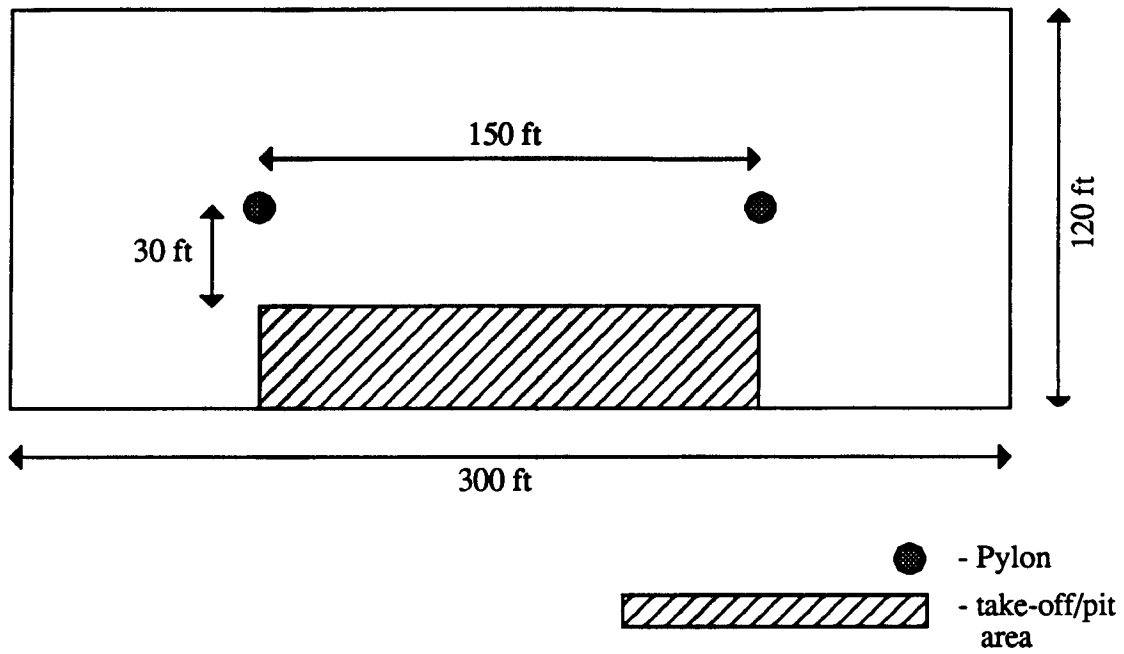
The system design shall satisfy the following.

- a. All basic operation will be line-of-sight with a fixed ground based pilot, although automatic control or other systems can be considered.
- b. The aircraft must be able to take-off from the ground and land on the ground.
- c. The aircraft must be able to maximize the loiter time within a restricted altitude range on a figure "8" course with a spacing of 150 ft between the two pylons which define the course.
- d. Ground handling and system operation must be able to be accomplished by two people.
- e. The complete aircraft must be able to be disassembled for transportation and storage and fit within a storage container no larger than 2' x 2' x 4'.
- f. Safety considerations for systems operations are critical. A complete safety assessment for the system is required.

#### **SPECIAL CONSIDERATIONS FOR THE TECHNOLOGY DEMONSTRATOR**

- a. The Technology Demonstrator will be a full sized prototype of the actual design.
- b. The flight tests for the Technology Demonstrator will be conducted in the Loftus Center on a closed course similar to that described above. The Demonstrator will be required to complete 3 laps on the course. The altitude must not exceed 25' at any point on the course.
- c. Take-off must be accomplished within the 150' take-off region shown on the following figure.
- d. Loiter time will be based on the time needed to complete the 3 complete laps in the air.
- e. The design team must make provisions for estimating altitude and flight speed during the tests. This information is to be monitored from ground based observers.
- f. The propulsion system for the technology demonstrator must not contain any chemicals or any other substance which could prove harmful to the Loftus Center or the aircraft operators.
- g. The radio control system and the instrumentation package must be removable and a complete system installation should be able to be accomplished in 30 min.

- h. System control for the flight demonstrator will be a Futaba 6FG radio system with up to 4 S28 servos or a system of comparable weight and size.
- i. All FAA and FCC regulations for operation of remotely piloted vehicles must be complied with.



This document defines the general mission. Namely, a remotely-piloted airplane is to take-off within a 150 ft x 30 ft area, fly at an altitude no greater than 25 ft, complete a series of three “figure-eight’s,” and land safely within the same area from which it took off. This obviously requires that the plane be capable of turning in both directions and have both longitudinal and lateral stability and control. Furthermore, because the plane will be flying inside the confines of a building, the propulsion unit must not be of a chemical nature. Safety considerations are a primary concern. Further constraints on the final design are dictated by the need disassemble the plane for storage and transportation. But aside from the actual flight course requirements and physical limitations, the primary mission goals are to fly at as low a Reynolds number as possible, and to maximize the loiter time (by flying as slow as possible). It is the attainment of these two goals which guided the overall design process.

In an effort to further quantify the mission, several additional constraints and refinements were made. First, based on the fact that the mean-wing-chord Reynolds number is defined as  $Re_c = \rho U c / \mu$ , a list of several mean chord length/flight speed combinations which correspond to a target Reynolds number of  $1 \times 10^5$  was produced. From this list it was finally decided that a cruise velocity of 25 ft/s could be attained and would adequately satisfy the primary mission goal of maximizing the loiter time. Dictated by this choice of Reynolds number and flight speed, a mean aerodynamic chord of 7.8 in was selected.

Secondly, some particular performance characteristics of the airplane were defined. A cruise altitude of 20 ft was chosen because it would allow for some leeway with the maximum ceiling of 25 ft. It was also determined that a minimum turning radius of 45 ft would be a good limit in regard to the “figure-eight” course. Furthermore, due to the relatively large size of the turns, it was desired to have enough excess power to sustain steady, level flight through the turn, or at the very least to keep the loss in altitude under 5 ft. Concerning the take-off procedure, it was decided that the plane should attain take-off speed and lift-off from the ground within a distance of 75 ft, and continue its ascent to cruise altitude in a total distance no greater than 150 ft.

Finally, because of the ban put on the use of chemical propulsion systems, it was decided that an electric motor/propeller combination would best fulfill the mission requirements. Two other possibilities were considered, however. Namely, mechanical storage (i.e. rubber band power) and some type of CO<sub>2</sub>-powered propulsion system. These were both rejected on the grounds that they would prove to be too unreliable and most likely not be able to operate continuously over the necessary time interval.

## II

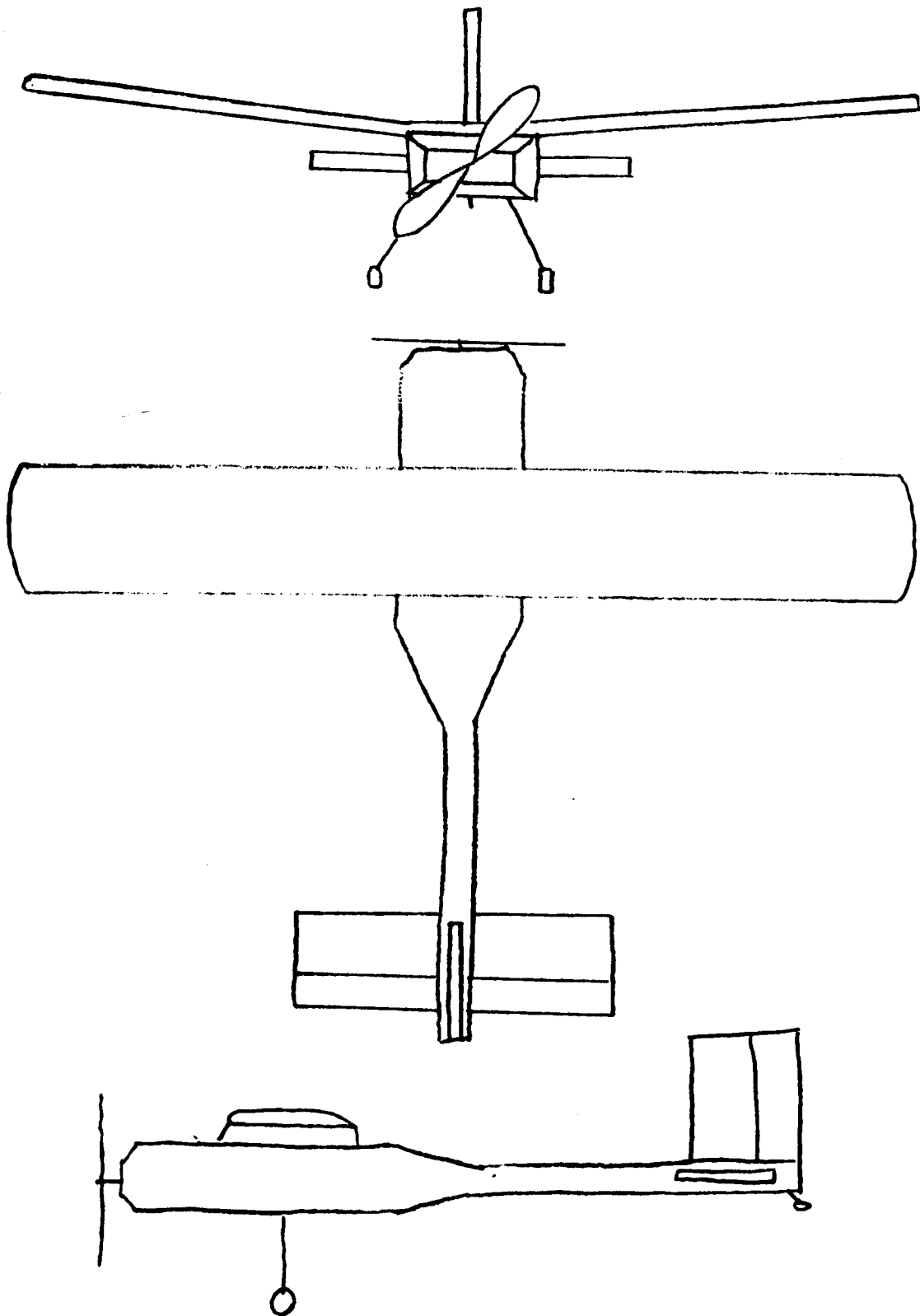
# Concept Selection Studies

Before anything else happens in the long process of building an airplane, a concept of what it will look like has to be considered. In deciding what the plane will be, many items have to be weighed against one another; what the plane will look like, the cost, the ease of construction, and the ease of flying are just four of the many characteristics of the airplane that must be balanced against one another before any real designing can be done. Design group E basically had only two designs to choose from: a conventional aircraft, and a canard aircraft.

The conventional aircraft envisioned was a powered sailplane with a long wingspan, long body, and small fuselage. One team member's concept of this design can be seen in Fig. 2.1. This airplane would not be too difficult to design, because most of the information available on designing aircraft is specifically for conventional aircraft. The conventional aircraft design had two drawbacks. First, the wing would have to generate more lift than the aircraft weighed, due to the fact that the horizontal tail would have to generate negative lift to keep the airplane stable and controllable. Second, almost every other group was using a conventional design; this plane would be just another conventional design flying around in a figure-eight.

The canard airplane was just a basic canard design: low mounted canard, high mounted wing, and a pusher-prop. This plane had several advantages. First, it would be different; no other airplane was using a canard. Second, it would be interesting to design and build; besides, most aircraft designed commercially are conventional, not canard users. Finally, the

**FIGURE 2.1** Three-View Drawing of Conventional Design





initial concept looked very futuristic, and to several group members, aesthetics were very important. The primary drawback of the canard airplane is that it is different; many of the equations used to design an aircraft, and almost all of the stability and control equations, would have to be adapted to a canard design.

After much discussion, the canard proponents won the discussion. Everyone agreed that it would be interesting to design an aircraft that would be different from everybody else's. Another benefit was that it would use two surfaces for lift instead of just one as the conventional ones do. Also, the plane would just turn with the rudder instead of with ailerons; this would make it easier to fly, and cut down on the weight because of fewer moving parts. In addition, the pusher-prop was changed to a tractor because the pusher-prop was found to be very inefficient. Finally, the fuselage was enlarged because the initial one would not have been able to suffice after the other changes that were made to the airplane.

# III

## Aerodynamic Design

### 3.1 Wing Selection

The procedure to size the wing followed primarily from the design parameters that guided the entire project. Of these, the greatest effect on the wing is felt from the Reynolds Number requirement of  $10^5$ . Since the Reynolds Number is a function of the chord, velocity, and dynamic viscosity, and the dynamic viscosity is constant, either the chord or the velocity must be known in order to calculate the other. A velocity of 25 ft/s was set. From the definition of Reynolds Number, the chord is 0.648 ft. Next, the available data base of aircraft from past research at the University of Notre Dame was searched in order to find an approximation for  $C_{L_{max}}$ ; this resulted in an average  $C_{L_{max}}$  of 1.0. (This value was later confirmed for the final wing using lifting line theory by increasing angle of attack until wing stall occurred; a value of 1.02 resulted from these calculations.) The  $C_L$  was arbitrarily set at 0.7 as a compromise between one with a safe margin before stall occurs, and one that would be so big as to be impractical. Since  $C_L$  depends on air density, velocity, lift, and surface area, once the required lift was known, the surface area of the wing could also be calculated.

The lift for this airplane would differ from conventional airplanes because it utilizes a canard as opposed to the normal horizontal tail. This means that the wing only has to carry a fraction of the lift, instead of all of it as the conventional designs must. A distribution of lift of 70% - 30% between the wing and canard was decided on. This reflects a compromise between a tandem wing design and a normal canard which uses at most a 80% - 20% split. On one

hand, the wing has to carry less lift, therefore it can be smaller. On the other hand, the canard could become so big that any loss of lift on the canard could send the plane nosing into the ground. It was felt that with a 70% - 30% split of lift the second problem could be reduced by limiting the range of canard motion to just a few degrees in either direction.

At this point, all that is needed is the weight of the airplane to finish calculating the dimensions of the wing. It was determined that the entire airplane would weigh 2.3 lb, of which 0.69 lb would be lifted by the canard, and 1.61 lb would be lifted by the wing. This value would be increased to 1.7 lb due to the fact that the dihedral would cause the wing to lose approximately 5% of its lifting force. From the definition of lift as a function of  $C_L$ , velocity, air density, and surface area, the surface area has to be 3.24 ft<sup>2</sup>; since the chord is 0.65 ft, the wing span must be 5 ft. The wing is rectangular primarily because of the ease of construction.

### 3.2 Airfoil Selection for the Wing

The airfoil chosen for this plane is the Clark-Y. The Clark-Y has been used for many years in low Reynolds number applications; in other words, it has proven reliable in the conditions that this airplane will be flying in. The primary reason for deciding on this airfoil is its low drag values over the entire range of  $C_L$ 's that the plane will fly through. This is important because in order to reduce weight, it was decided to use a smaller engine with fewer batteries; hence, the drag has to be minimized or else the engine would not pull the plane through the air. As stated above, the wing needs a  $C_L$  of 0.7. Even after the effects of a finite wing are accounted for, the wing made from the Clark-Y still has a comfortable range of 6° of attack angle before stall occurs (cruise  $\alpha=4^\circ$ , stall  $\alpha= 10^\circ$ ). Although the margin of error would be greater using an airfoil with a higher  $C_{L_{max}}$  (for example, the Wortmann FX63-137B, which has the best  $L/D$  of any other airfoil inspected), the Clark-Y has the lowest drag of any airfoil. (Refer to Fig. 3.2.2 for the drag polar for the Wortmann FX63-137B) Also, with its thick trailing edge it would be easier to construct than the Wortmann.

**FIGURE 3.2.1 Drag Polar for Clark-Y**

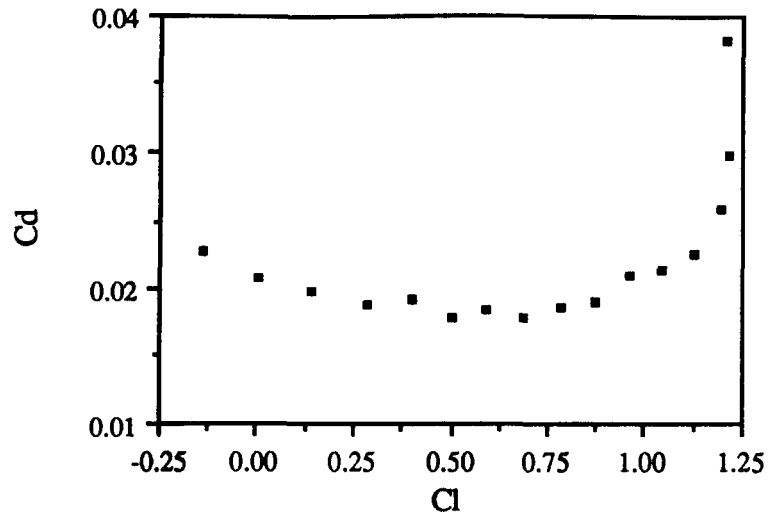
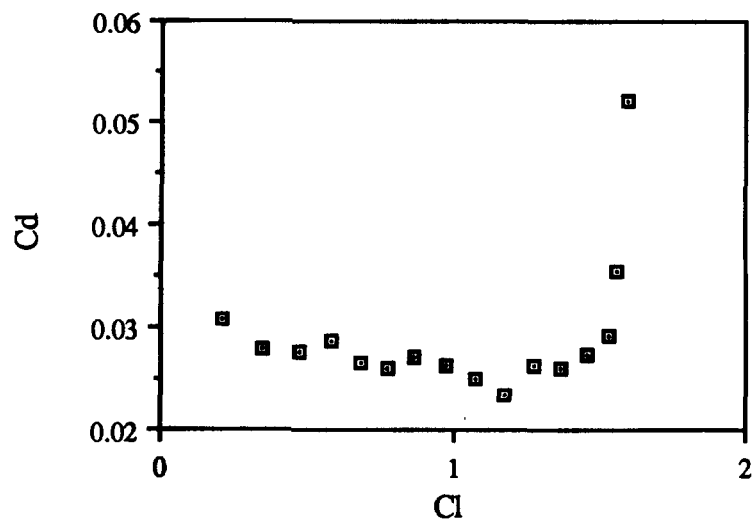


**FIGURE 3.2.2 Drag Polar for Wortmann FX63-137B**



### 3.3 Canard Sizing

Unlike the wing, the canard is not governed by the design requirements; in other words, it can be made any size, so long as the chord does not exceed 0.65 ft. The only other constraint is

that it must lift 0.69 lb. The airfoil section chosen for the canard is the Clark-Y for two reasons. Firstly, it is already being used with the wing, and secondly,  $C_l$  and  $C_d$  data was available for Reynolds numbers down to  $6 \times 10^4$ . Next, the chord was set at 0.5 ft because it resulted in a Reynolds number of  $7.7 \times 10^4$ , which has information available; also 0.5 is an easy number to calculate with. The span was set at 2.8 ft because with these values the Aspect Ratio is greater than 5. This is important, because the equations in dealing with finite wings (lift curve slope, drag, etc.) are only applicable for Aspect Ratios greater than 5. The canard is rectangular, like the wing, and has no dihedral. The canard has a  $C_L$  of 0.7 at cruise, and stalls at an angle of attack of  $9^\circ$ . This is important because it insures that the canard will stall before the wing, which is one of the desirable characteristics of a canard aircraft.

### 3.4 Aircraft Aerodynamics

The  $C_L$  for the entire aircraft was found by first calculating the required  $C_L$  at cruise (1.0). Next, the information on the airplane was entered into the computer program LinAir. LinAir does not calculate exact values, but does find trends such as the lift curve slope and efficiency with much precision. From this program, it was determined that the lift curve slope ( $C_{L\alpha}$ ) is 0.097 per degree, and the Oswald Efficiency Factor is 0.86. Figure 3.4.1 shows the lift curve which was computed by the LinAir program. The zero lift angle of attack for the airplane is  $-4.95^\circ$ , and the stall angle for the airplane is  $7.4^\circ$ .

The parasitic drag coefficient is 0.035; this is found from adding together the parasitic drags from the wing, canard, fuselage, and tail, then basing the drag coefficient on the wing. The induced drag is derived from the lift. The drag vs. angle of attack curve for the aircraft is shown in Fig. 3.4.2 and the drag polar for the whole aircraft is shown in Fig. 3.4.3.

**FIGURE 3.4.1** The Dawdler's Lift Curve

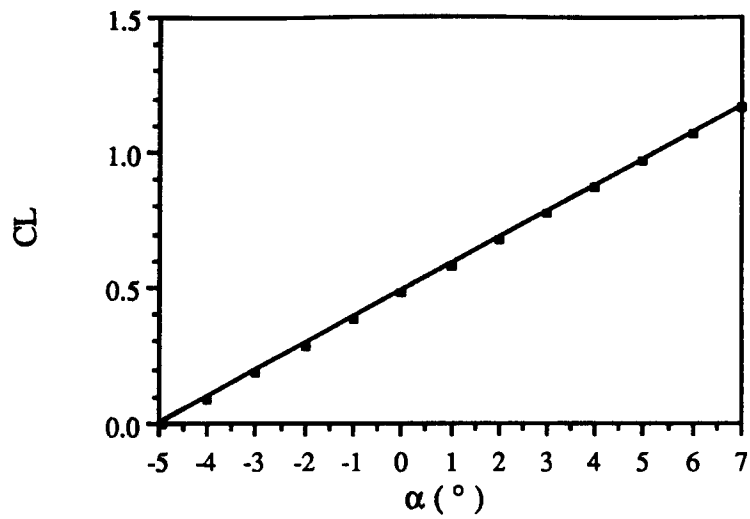


**FIGURE 3.4.2** Drag Coefficient vs. Angle of Attack of the Whole Aircraft

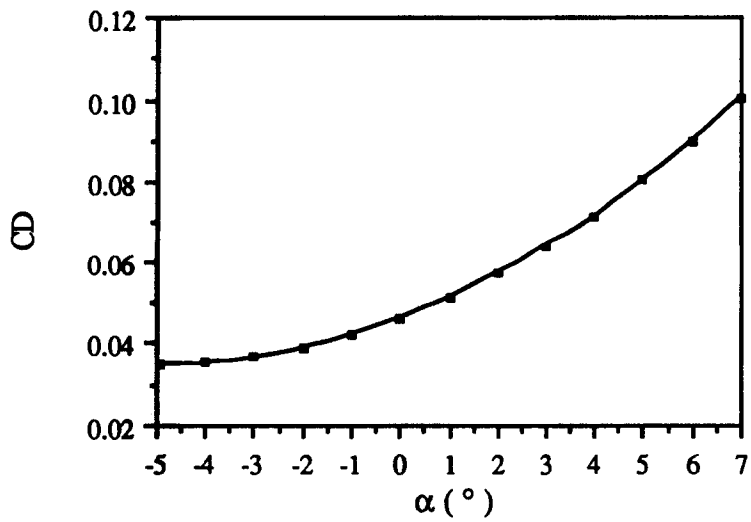
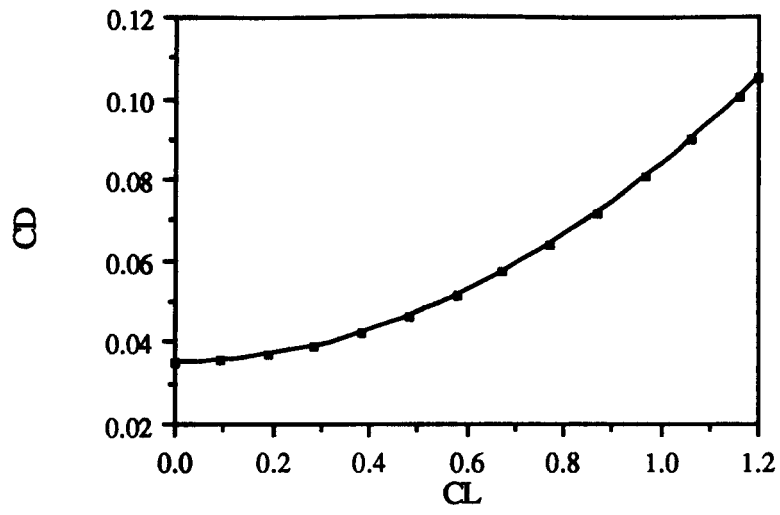


**FIGURE 3.4.3 Drag Polar for the Entire Aircraft**



## IV Propulsion System

### 4.1 System Selection

The mission specifications requires that the propulsion system for the RPV design be non-airbreathing and not emit any mass. This type of system would be able to operate in environments with little or no oxygen such as very high earth altitudes or even another planet's atmosphere without causing any contamination or pollution. These requirements rule out several conventional propulsion systems such as rockets and reciprocating propeller engines. Two types of systems that did meet the requirements and were considered were a rubber band powered propeller system and an electric motor/battery powered propeller system.

The rubber band power system would use the stored mechanical energy of a twisted rubber band or rubber tubing to drive a propeller. This type of system could be very lightweight and inexpensive, but problems were predicted in being able to provide any engine speed control. It might be possible to develop a mechanism that could apply a friction force to the propeller gear to control the speed of rotation, however, no information could be found on such a system, and it was abandoned.

The electric motor/battery power type systems were found to be readily available commercially and capable of providing the power necessary for the mission. Information was available from several model airplane advertisements and brochures in the form of maximum power ratings for most electric motors, while two motors even had tables of current drawn, gear power, and torque for various motor speeds. These motors were the Astro 05 and Astro



15.[1] Many types of engine control systems are also available for the electric motor systems and are ideally suited to the mission objectives. Because of the availability of electric motor systems and engine control systems along with a useful data base, this type of system was chosen for the design.

## 4.2 System Integration

The Dawdler uses a single motor that is mounted in the front of the fuselage with a tractor type propeller. A single engine is used primarily because it can provide the power necessary for steady level cruise and enough excess power for a moderate rate of climb. The use of two engines would greatly add to the propulsion system weight and would require more battery capacity than a single engine. The only benefit derived from using two motors would be that by having them counter-rotate, the net roll moment created by the propeller torque would be zero. However, proper geometric wing twist can easily be implemented to counteract the nonzero moment created by a single engine system.

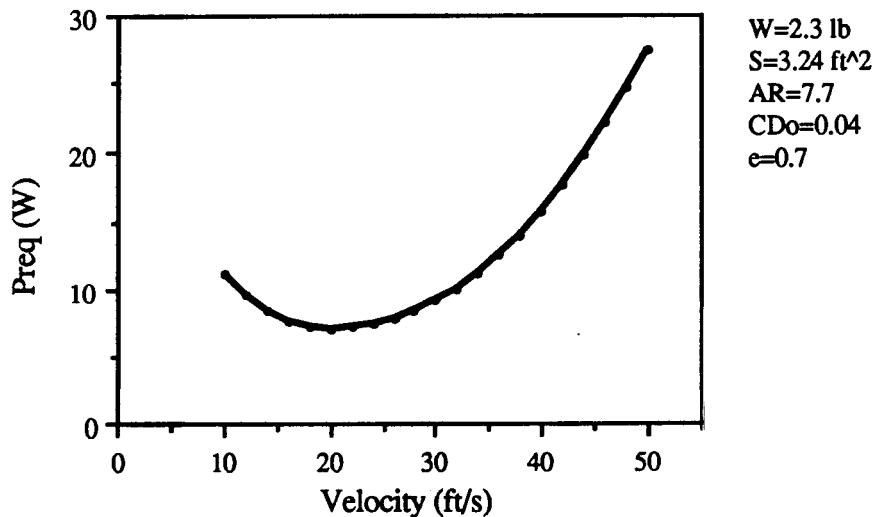
The decision to use a forward mounted tractor type propeller stemmed from the design objective to have an aircraft that would make "tail dragger" type landings. This would reduce the weight of the landing gear since only two gear would be needed versus three. The forward placement of the propeller would allow the thrust line to be located near the longitudinal cg axis without requiring large landing gear to maintain ground clearance during landings.

A second possible benefit of having the propeller in front of the fuselage is a slight increase in lift from the front wing. The increased velocity in the slip stream of the propeller will pass over the canard which is located fairly close behind the propeller. The increase in dynamic pressure should provide an increase in lift at the root portion of the canard. Unfortunately, the flow behind the propeller is very turbulent and rotational losses in the flow could lessen the benefit of higher local velocity. Ideally, experimental tests should be performed to verify the predictions.

### 4.3 Motor Sizing

Because the mission objective includes the use of a powered cart to accelerate the RPV up to a speed which will allow it to take-off and perform a decelerated climb up to the design altitude of 20 feet, the on-board propulsion system is only required to provide enough power to maintain steady level flight at the desired cruise speed of 25 ft/s and enough excess power to allow a small climb capability to compensate for any losses in altitude. This was a major factor in the initial sizing of the aircraft propulsion system. Since the take-off is the most demanding part of the mission, it was possible to reduce the size of the motor and therefore the weight of the entire design.

FIGURE 4.3.1 Power Required Estimate for the Dawdler



The following parameter values were used for all of the propulsion calculations:

$$\begin{aligned} W &= 2.3 \text{ lb} & C_{D0} &= 0.04 \\ S &= 3.24 \text{ ft}^2 & e &= 0.7 \\ AR &= 7.7 \end{aligned}$$

The drag polar was estimated from the relation

$$C_D = C_{D_0} + C_L^2/(\pi A Re)$$

and the values for  $C_{D_0}$  and span efficiency factor,  $e$ , were suggested by several sources. From the preliminary estimates of the total design weight, lifting surface areas, and drag polar, it was possible to calculate the power required for level flight over a range of velocities (see Fig. 4.3.1). A conservative estimate of 10 watts was made for the minimum  $P_{req}$  for level flight at 25 ft/s. This was used as a criterion for the cut-off value of  $P_{av}$  max that the system would absolutely have to supply to be considered. Making another conservative estimate of 40% for the propeller efficiency, the maximum power ratings for several motors were used to select the proper motor size as shown in Table 4.3.1.

**TABLE 4.3.1** Motor Specifications and Predicted Power Available

Astro Motor	NiCad Battery	system weight	max Pav from shaft	predicted max $P_{av}$ from prop
Cobalt 020	4x800 mah	9 oz	50 watts	20 watts
Cobalt 035	5x800 mah	11 oz	90 watts	36 watts
Cobalt 05	7x900 mah	16 oz	125 watts	50 watts
Cobalt 15	12x900 mah	25 oz	200 watts	80 watts

Although the Astro 020 motor was predicted to be able to provide enough power, the extra power of the 035 motor was considered more beneficial than the penalty of an extra two ounces in system weight. The Astro 035 motor should be able to supply an adequate amount of power for the design objective at a relatively low weight and was selected for the Dawdler design. Recall that the Dawdler mission will utilize a powered cart during take-off, allowing for such a small motor. Ordinarily the power required during take-off is at least twice that required for cruise.

#### 4.4 Propeller Design

The Master Airscrew 9-6 propeller was chosen for the Dawdler propulsion system. The choice of this propeller was based on results obtained from blade-element theory and comparisons made with experimental data from wind tunnel tests.[2] This combination of 9" diameter and 6" pitch proved to provide the best efficiency at the cruise velocity and good off-design characteristics.

A computer program developed by B.N. Young was used to make the blade-element theory predictions of the thrust coefficient, power coefficient, and propeller efficiency.[3] These results were only approximate since simple blade-element theory assumes inviscid flow. However, with corrections for induced velocity and tip losses accurate results have been obtained for some propellers.[3] The low Reynolds numbers experienced in this particular mission might cause these estimates to be even less accurate. Young's program does contain a correction for Re, but it is still believed that the coefficients are overestimated.

Experimental results tended to vary from the theoretical results with respect to the efficiency curves (see Fig. 4.4.1), but direct correlations are difficult to make because the propellers were of different sizes and makes. It is believed, though, that the theoretical results overestimated the values of eta and predicted the location of the peaks at too large of values for the advance ratio J. Accounting for this fact and because the most efficient engine speed is known to some degree, the relation  $J=V/(nD)$  suggests that the propeller should have its maximum efficiency in the range of  $0.25 < J < 0.45$  (depending on the diameter) to be best suited for this mission. A 6" propeller pitch is predicted to be the best choice from the data of Fig. 4.4.1.

The selection of the propeller diameter was made from an analysis of the useful power available from the propeller and the power required to turn the propeller, or  $P_{gear}$ . Using the results for  $C_p$  and  $C_t$  from Young's program, another computer program DESPWR was developed to calculate  $P_{av}$  and  $P_{gear}$  from the equations:

$$P_{av} = \text{thrust} \times \text{velocity} = (C_t \rho n^2 D^4) V$$

$$P_{\text{gear}} = \text{torque} \times \omega = C_p \rho n^3 D^5$$

Both quantities have a strong dependence on  $D$ , the propeller diameter. Results are given in Table 4.4.1. It can be seen that a diameter of 9" supplies the necessary  $P_{\text{av}}$  to cruise at 25 ft/s at the least value of  $P_{\text{gear}}$ . This means that the motor will be drawing less current from the battery for a 9" propeller than it would if it had to turn a smaller propeller at a faster rate or a larger propeller at a slower rate. Therefore, the best choice of diameter appears to be approximately 9 inches.

**FIGURE 4.4.1** Variation of Efficiency Curves with Pitch

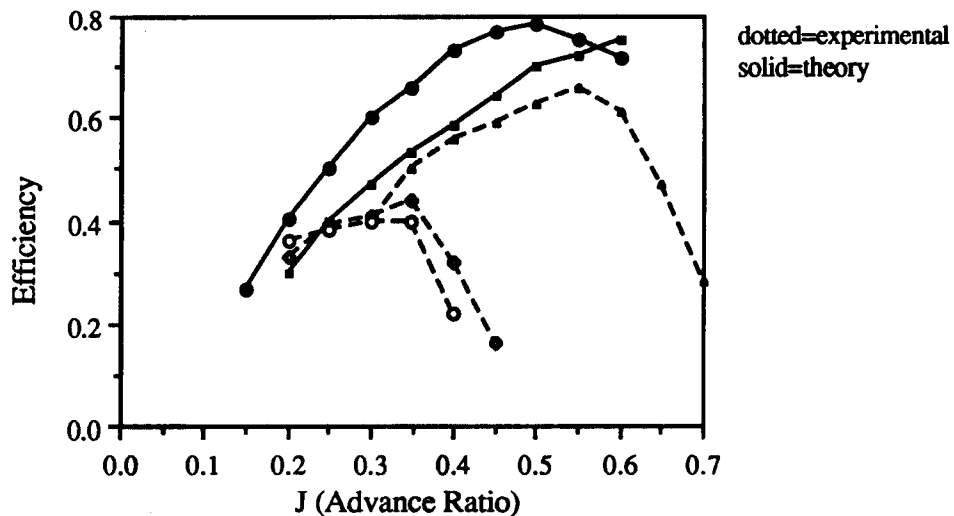


**TABLE 4.4.1** Motor Performance for Several Prop Diameters  
(pitch = 6 in ,  $V = 25$  ft/s ,  $P_{\text{av}} = 7.6$  watts)

Propeller Diameter	power required to turn gear	applied voltage	current drain	rpm
6 in	14.6 W	8.1 V*	6.1 Amp	9000
8 in	12.9 W	5.3 V	8.1 Amp	5400
9 in	12.6 W	4.6 V	9.3 Amp	4450
10 in	12.6 W	4.1 V	10.6 Amp	3750
12 in	13.8 W	3.8 V	14.4 Amp	2900

\* above recommended voltage

A two blade propeller was selected for the design for several reasons. First, it appears that two blade propellers are most popular for small, low-speed aircraft.[4] The biggest benefit from using a three or four blade propeller is a reduction in the noise output level. This is not a primary concern for the design of this mission. Secondly, the two blade propellers are available in many more styles and sizes than are the three and four blade propellers. Finally, a two blade propeller would weigh less.

#### 4.5 Propulsion System Performance Predictions

The total system performance of the Astro 035 motor coupled with a Master Airscrew 9-6 propeller was predicted using the results obtained from the propeller analysis and estimations of the motor's characteristic constants. These constants include the motor torque coefficient  $K_t$ , speed coefficient  $K_v$ , and armature resistance  $R_a$ . These constants were scaled from comparisons with the 05 and 15 size motors, and were estimated at  $K_t=0.54$  in-oz/A,  $K_v=0.000351$  V/rev, and  $R_a=0.05$   $\Omega$ . It was also assumed that there would be a constant torque loss due to friction of 1.0 in-oz and a gear efficiency of 0.95. These values were used in another computer program DESPR2 to calculate the current, voltage,  $P_{av}$ , and  $P_{gear}$  for various flight velocities and motor speed settings. The figures of merit of concern for the system were the maximum power available and the current draw at cruise. Also of interest were the maximum propeller rpm and voltage settings for different flight conditions.

It was necessary to include a gear box with the motor once the decision to use a 9 inch propeller was made. This allows the propeller to turn at a slower rate than the motor armature. Only one gear ratio was available for the Astro 035 motor — 2.4 to 1. With the geared propeller, the motor can run at a more efficient speed giving the overall system better performance.

The power available curves are shown superimposed on the Dawdler's predicted  $P_{req}$  curve in Fig. 4.5.1. The maximum power available of the system is predicted to be about 20

watts. This occurs at a flight speed of 32 ft/s and propeller speed of 6200 rpm. The propeller cannot turn any faster than this because of the voltage constraint. The applied voltage is recommended to be no more than 6.75 volts. If a higher voltage were applied, the motor still would not be able to turn the propeller more than 7000 rpm because the system is constrained to a maximum current of 20 A. A 20 amp fuse is included in the system to prevent damage to the motor.

**FIGURE 4.5.1** Power Available for Master Airscrew 9-6

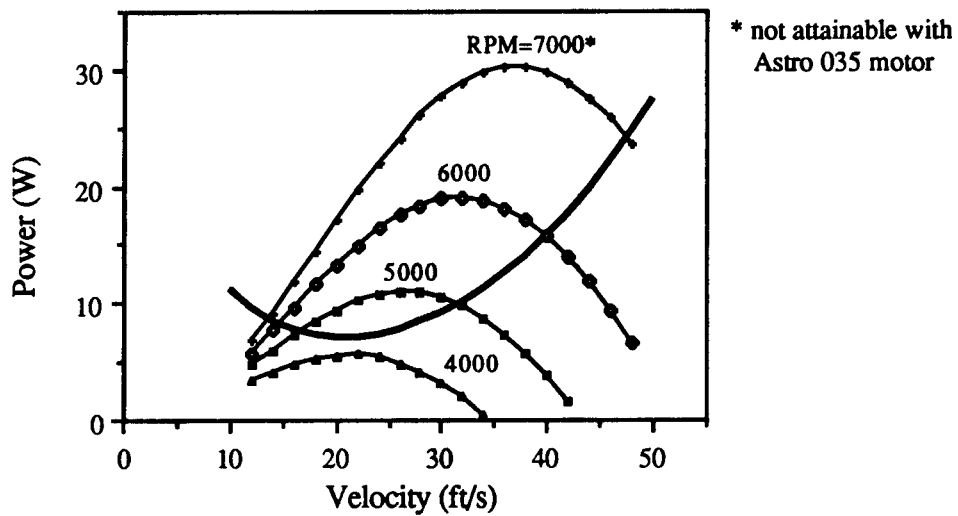
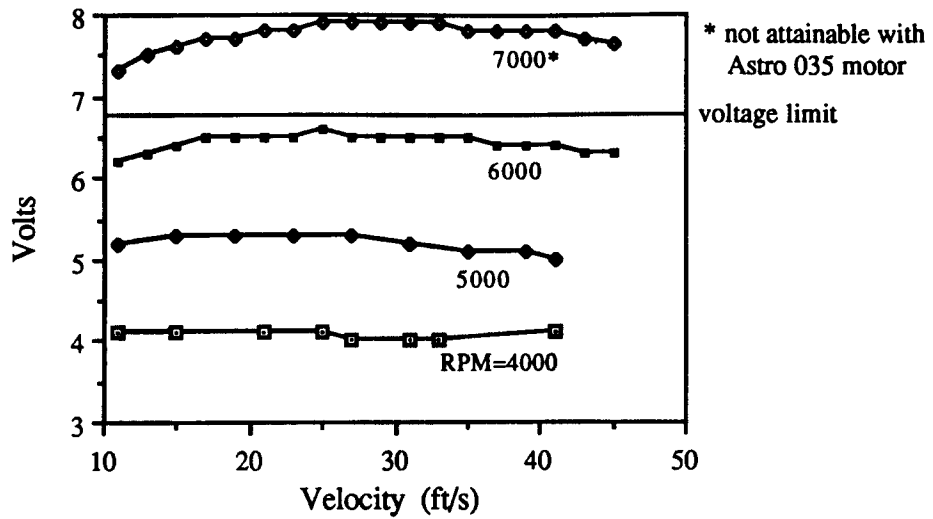


Figure 4.5.2 shows the voltage settings required for several motor speeds. Figure 4.5.3 shows the current draw of the motor for the same settings. From these two figures and Fig. 4.5.1, it can be seen that the applied voltage must be about 4.7 volts at cruise which corresponds to a propeller speed of 4450 rpm and current drain of 9.3 A. With this in mind, it is estimated that the system will consume about 275 mah of battery capacity during the mission. 500 mah NiCad cells were selected to provide the necessary endurance required by the mission for the least amount of battery weight.

**FIGURE 4.5.2** Battery Voltages at Several Speed Settings  
(Astro 035 Motor With Master Airscrew 9-6 Propeller)



**FIGURE 4.5.3** Current Draw by Master Airscrew 9-6 Propeller at Set RPM

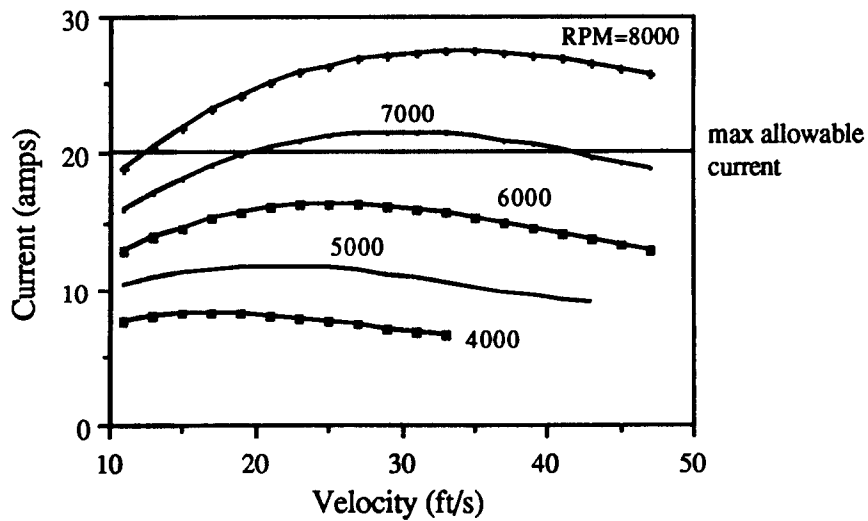


Figure 4.5.1 also indicates that the maximum velocity the Dawdler can achieve is about 40 ft/s. The maximum excess power ( $P_{av} - P_{req}$ ) the system can supply is approximately 10 watts at a velocity of 29 ft/s. From this, the maximum rate of climb given by the expression



$R/C=(P_{av}-P_{req})/W$ , where  $W$  is the total weight of the Dawdler (2.3 lb), is predicted to be 3.2 ft/s. Table 4.5.1 summarizes the important performance predictions.

**TABLE 4.5.1** Summary of Performance Predictions

<u>System</u>	Astro Cobalt 035 motor (2.4:1 gear reduction) Master Airscrew 9-6 propeller 5 x 500 mah NiCad cells (6.75 Volts)
	Total system weight = 11.3 oz
Max $P_{av}$ = 20 W @ 6200 rpm	voltage at cruise = 4.7 Volts
Max velocity = 40 ft/s	current at cruise = 9.3 Amps
Max Rate of Climb = 3.2 ft/s	rpm at cruise = 4450
Max propeller speed = 6200 rpm	

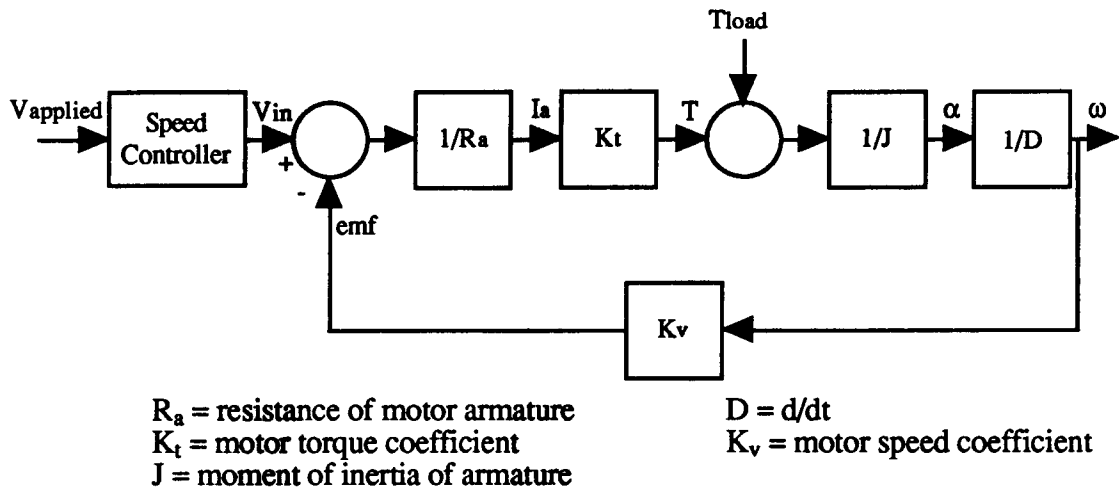
#### 4.6 Engine Control

In order to properly control the speed of the airplane, the system must include some sort of engine control. Since the engine speed is controlled by the applied voltage, it would be possible to fix the voltage at one setting and let it go, but the airplane would sink if the voltage was set too low (if it ever even got off the ground), or would fly too fast if the voltage was set too high. There would be no way to adjust the throttle for different flight conditions — a serious obstacle to the successful completion of the mission. To fix this, the design will include an electronic speed controller.

Because the flight conditions will change throughout the mission, i.e. initial climb, level cruise, and turning maneuvers, the load torque applied to the propeller will change also. The motor speed is a function of both the voltage applied to the motor and the load torque experienced by the propeller. A block diagram for the control of the electric motor speed is shown in Fig.4.6.1. Since the load torque will be different for separate parts of the mission, the applied voltage must also be changed in order to maintain the desired response, the engine

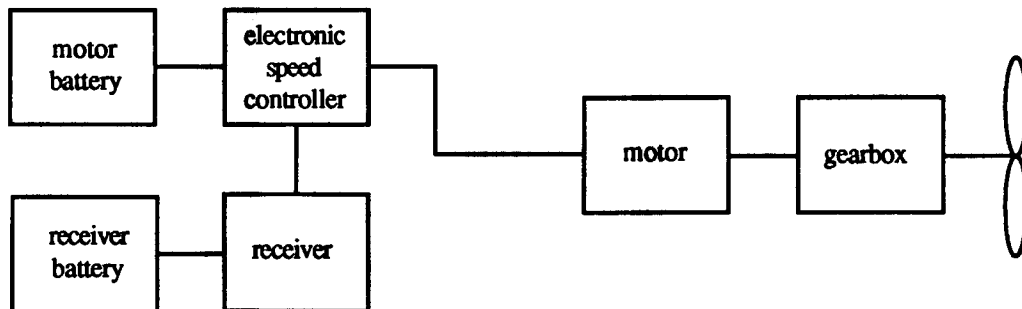
speed. Note that all of the other constants are fixed characteristics of the motor itself. The electronic speed control will allow the applied voltage to be changed appropriately during the flight.

**FIGURE 4.6.1** Block Diagram of Engine Control System



The speed controller is essentially an electric on-off switch connected in series between the propulsion battery pack and the motor. The controller is itself controlled through one of the receiver's radio channels. The pilot can select the speed with the position of a joystick. By switching the current to the motor on and off many times a second, the speed controller regulates the effective voltage seen by the motor and therefore the speed at which the motor runs. A schematic diagram of the propulsion system is shown in Fig. 4.6.2.

**FIGURE 4.6.2** Schematic Diagram of Propulsion System



The disadvantages of this type of engine control are its high cost and its additional weight to the total propulsion system. The electronic controller costs nearly 50% more than the motor itself and weighs almost 50% as much. However, as mentioned before, without this control the mission objectives would be very difficult to accomplish.

## V Weight Estimation

### 5.1 Weight Percentages

The weight of the Dawdler was calculated by analysis of all of the components of the aircraft propulsion system, control system, and structures. The weights of all components were estimated by using data bases from past projects as well as information from the engine company and radio control system information. Structure weights were estimated using weights of similar projects currently on display in the Aero Lab. From these estimates, our preliminary weight of 36.8 oz was determined. Once the actual equipment was acquired, the system components were weighed and a more accurate estimation was made. This included estimating the actual weight of the structure by analysis of the framework and required structural reinforcements. All these calculations were based on the average densities of the structural material property (see Table 5.1.1). The information was acquired by experimentation with various woods and was provided to us so the reference is unknown. However, the density information was checked with samples of materials and was determined to be accurate. Volumes for each piece of structure and its corresponding density were used to determine the structure weight. The measured and estimated component weights are listed in Table 5.1.2. The total system weight has been determined to be 37.2 oz. This is quite close to the estimated weight of 36.8 oz. The slight discrepancy will hopefully be eliminated during the construction as some overestimates were made in the structure sizing.

**TABLE 5.1.1 Material Properties**

Material	E(psi)	$\rho$ (lb/in <sup>3</sup> )	$\sigma_{xx}$ (psi)
Balsa	65E03	0.0058	400
Spruce	1.3E06	0.016	6200
Birch Plywood	2.01E06	0.0231	2500
Aluminum	1E07	0.100	20E03

**TABLE 5.1.2 Component Weights**

Component	Weight (oz)	Wt. Fraction (%)
Engine, Engine Mount	7.764	20.9
Engine Battery	3.800	10.2
Receiver, Servos, System Battery	4.348	11.7
Speed Controller	1.605	4.3
Wing	8.376	22.5
Canard	3.700	9.9
Fuselage	4.607	12.4
Landing Gear, Misc.	3.000	8.1
<b>Total System Weight</b>	<b>37.20</b>	

## 5.2 Center of Gravity Estimation

Once the component weights has been determined, the center of gravity must be estimated. This consists of the use of a simple mathematical equation evaluated with all of the vehicle components in mind. To find the most accurate center of gravity, the vehicle needs to be broken up into small components. These components consisted of the structural components, the radio equipment, propulsion system and speed controller. Locations for these components were selected due to the need for the center of gravity to reside in a specific location. This position is located at 15.25 inches from the nose of the aircraft. Refer to Fig. 5.2.1 for a description of the coordinate system. This position was selected for pitch stability. The equipment was placed into the aircraft as shown in Table 5.2.1. Note that for each component,

the position is that of the component's center of gravity. For the wings, this position was estimated to be the quarter chord point.

**FIGURE 5.2.1** Coordinate System

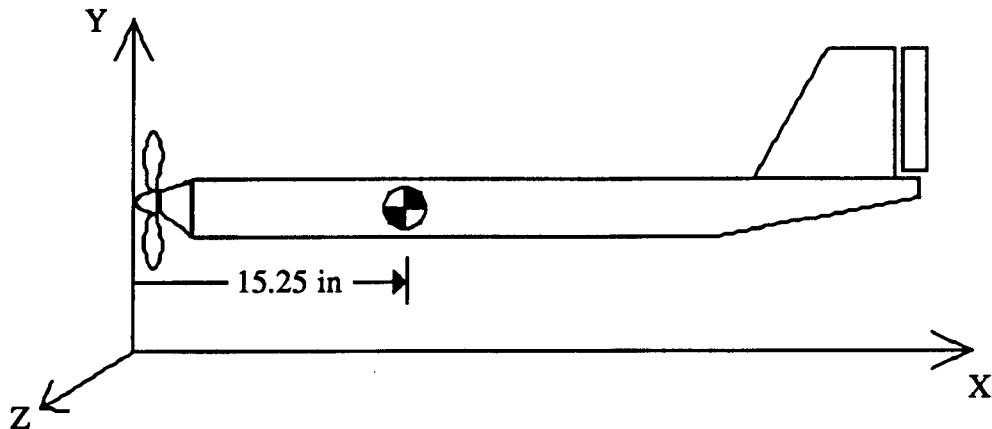


**TABLE 5.2.1** Component Placement and cg Location

Center of Gravity Locations		
Component	C.G. Location (inches)	Weight (oz)
Fuselage Hull	8.612	2.580
Vertical Stabilizer	33.500	0.580
Wing	27.000	8.376
Canard	6.000	3.700
Engine, Engine Mount	2.500	7.764
Engine Battery	20.000	3.800
Receiver	20.000	0.952
System Battery	21.000	2.092
Servo 1 (canard)	19.000	0.652
Servo 2 (rudder)	19.000	0.652
Speed Controller	15.000	1.605
<b>TOTAL AIRCRAFT</b>	<b>15.25</b>	<b>37.200</b>

It should be noted that the above estimates as to the locations of the equipment and structure is only an estimate until the exact structure weight is known. The above numbers will be valid if the structure can be built at the weight that is specified. Because of the distance between the engine and the engine battery, it will be required that a significant amount of wire be placed in the RPV. As this is a distributed load, it will not have a major effect on the location of the center of gravity, but will have a significant effect on the weight of the aircraft. The wiring weight and miscellaneous equipment weights (such as control horns, pushrods, etc.) are not included in the calculation of the center of gravity as they will not affect the location in a drastic fashion.

The location of the center of gravity is very sensitive to the location of the system and engine batteries. Because a significant portion of the vehicle weight is located in the engine, which is mounted on the front of the aircraft, the batteries must be located at the very rear of the vehicle. Because of this, the ability for the cg to travel rearward is severely limited. A need to locate the cg farther aft would require the use of ballast, causing an increase in vehicle weight. With the layout at present, the center of gravity is not able to move much further rearward without ballast. This will not be a problem as long as we can locate the items where we want to. If needed the center of gravity may be moved as far forward as required, since most of the payload area is not being used towards the front of the vehicle.

# VI

## Stability & Control

### 6.1 Lateral and Directional

Lateral and directional stability and control are maintained by the wing dihedral and the vertical tail and rudder. The critical condition for such control is the half circle turn of the figure eight maneuver. Our goal is to perform a steady level turn.

### 6.2 Wing Dihedral

The required wing dihedral was found through an analysis presented by Dr. Blaine Beron-Rawdon.[5] This article gives the required yaw angle for a steady state circle maneuver as a function of free stream velocity, circle radius and wing span. The yaw angle is a function of  $(1/S_w, b, W, 1/V^2, 1/r)$ . After correcting for the Dawdler's geometry and flight condition, the required yaw angle is 6-7°. The Dawdler will need a wing dihedral of 13°. Wing dihedral will reduce the effective lift of the wing proportional to the cosine of the dihedral angle. For a dihedral angle of 13° the wing will lose less than 3% of the lift provided by a flat wing.

### 6.3 Vertical Tail Sizing

The vertical tail and rudder were sized according to standard RC modelling rules.[6] The vertical tail size is given as:

$$S_{vt} = kS_w MAC/l_{vt}$$

where  $S_{vt}$  = vertical tail area



$S_w$  = wing area  
MAC = mean aerodynamic chord of the wing  
 $l_{vt}$  = distance between the cg of the plane and the ac of the tail  
 $k = 0.22$  for RC models.

For internal layout and weight balancing, the tail was placed 16 in behind the cg. The tail area is 49.4 in<sup>2</sup>.

The vertical tail is modelled as a flat plate. To keep the Reynolds number of the tail at 70,000, the chord of the vertical tail is 5.5 in. The span is 8.98 in. The tail has an aspect ratio of 1.63. For RC models it is desirable to have an effective aspect ratio ( $AR_e = 1.55AR$ )[5] of 2.5-3.0. The Dawdler has an  $AR_e = 2.53$ .

For adequate control, RC models should have rudders sized at 30-40% of the total tail area. The Dawdler's rudder is sized at 50% of the total tail to ensure adequate control.

#### 6.4 Stability Derivatives

For an aircraft to fly in a stable regime, its stability derivatives must have the following characteristics:

$$C_{m\alpha} < 0$$

$$C_{n\beta} > 0$$

$$C_{l\beta} < 0$$

The longitudinal stability derivative was solved for by the LinAir program which models the wing as a horseshoe vortex lattice in solving the Prandtl-Glauert linear partial differential equation. By varying the static margin and designating the trim angle of attack,  $C_{m_0}$  and  $C_{m\alpha}$  are found. For the Dawdler, it is desirable to have an  $\alpha_{trim}$  of 3°. Setting the static margin at 15% gives

$$C_{m_0} = 0.025$$

$$C_{m\alpha} = -0.0084 / \text{deg}$$

The lateral and directional stability derivatives were solved for by considering the contributions of each component of the aircraft. Appendix A contains a listing of the estimations of the component contributions. For lateral stability, the wing dihedral, vertical tail

and wing are all stabilizing elements. The canard alone is destabilizing. For directional stability, the fuselage is destabilizing while the wing, canard, and vertical tail are all stabilizing. For the Dawdler, the directional and lateral stability derivatives are:

$$C_{n\beta} = +0.012 / \text{deg}$$

$$C_{l\beta} = -0.007 / \text{deg}$$

The Dawdler, therefore, is flying in a stable regime. Figures 6.4.1, 6.4.2, and 6.4.3 give the pitching, rolling, and yawing moment coefficients as a function of angle of attack or sideslip angle.

**FIGURE 6.4.1** Pitching Moment Coefficient vs. Angle of Attack

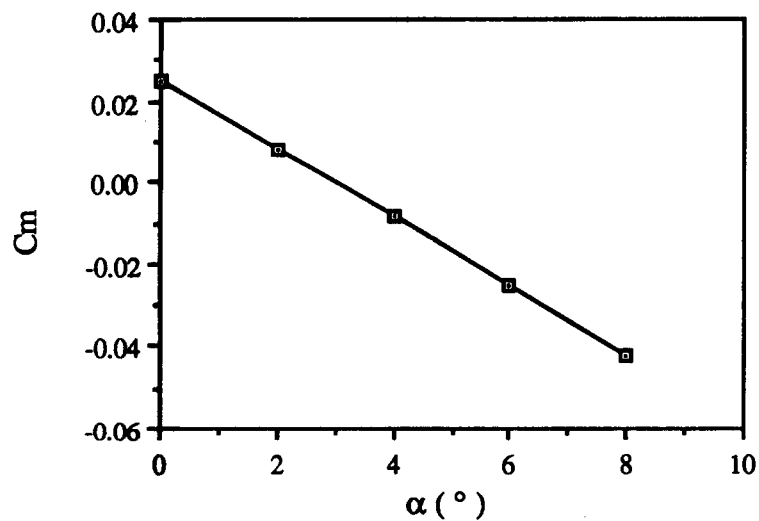


**FIGURE 6.4.2** Roll Moment Coefficient vs. Sideslip Angle

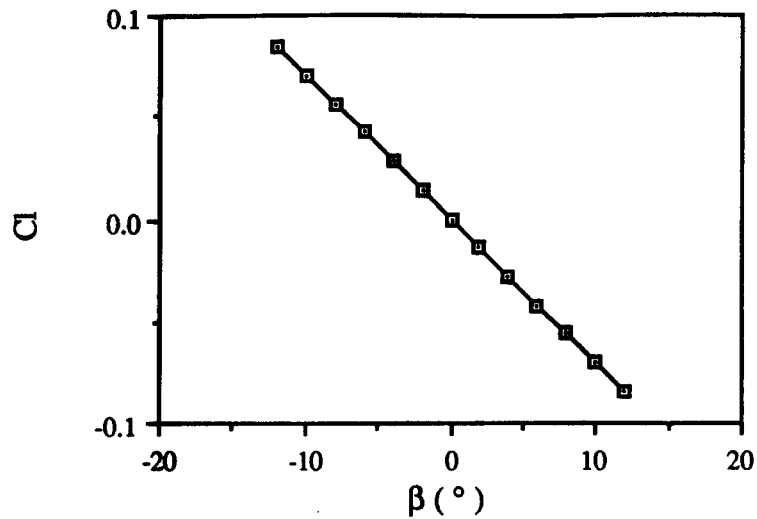
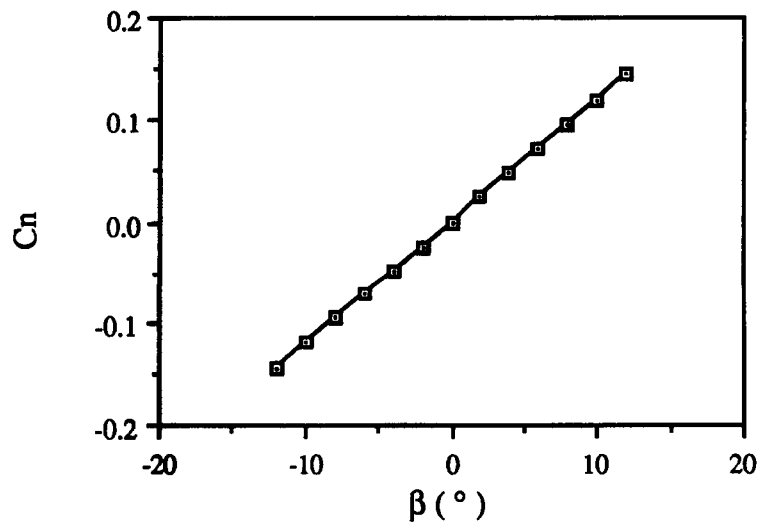


**FIGURE 6.4.3** Yaw Moment Coefficient vs. Sideslip Angle



### 6.5 Rudder Deflection

From the dihedral study, the maximum yaw angle the Dawdler will encounter is  $7^\circ$ . For no net yaw moment,  $C_n=0$ .  $C_n$  be expressed as

$$C_n = C_{n\beta}\beta + (C_n)_{\delta_r}\delta_r$$

Solving for rudder deflection ( $\delta_r$ ) such that  $C_n=0$  gives

$$\delta_r = -(C_{n\beta}\beta)/(C_n)_{\delta_r}$$

The term  $(C_n)_{\delta_r}$  can be expressed as[5]

$$(C_n)_{\delta_r} = -nV_v \frac{\partial C_{Lv}}{\partial \delta_r} \quad n = \frac{q_{vt}}{q}$$

and

$$\frac{\partial C_{Lv}}{\partial \delta_r} = \frac{\partial C_{Lv}}{\partial \alpha_v} \frac{\partial \alpha_v}{\partial \delta_r} = (C_{L\alpha})_{vt} \tau$$

where  $\alpha_v$  is the angle of attack the vertical tail “sees,” comprised of the yaw angle and sidewash angle. The term  $\tau$  is a function of rudder area ( $S_r$ ) versus vertical tail area.[6] For the Dawdler,  $S_r/S_{vt}=0.5$  and  $\tau=0.68$ . This gives  $\delta_r=16.2^\circ$ .

## 6.6 Longitudinal Stability

Longitudinal stability and control are maintained by a fully deflectable canard. The canard was sized for providing 30% of the total lift. For the wing to provide 70% of the lift, it must have an angle of attack of 6-7°. The wing is mounted at an angle of 4°, therefore the Dawdler must fly at  $\alpha_{trim}=3^\circ$ .

## VII

# Performance Estimation

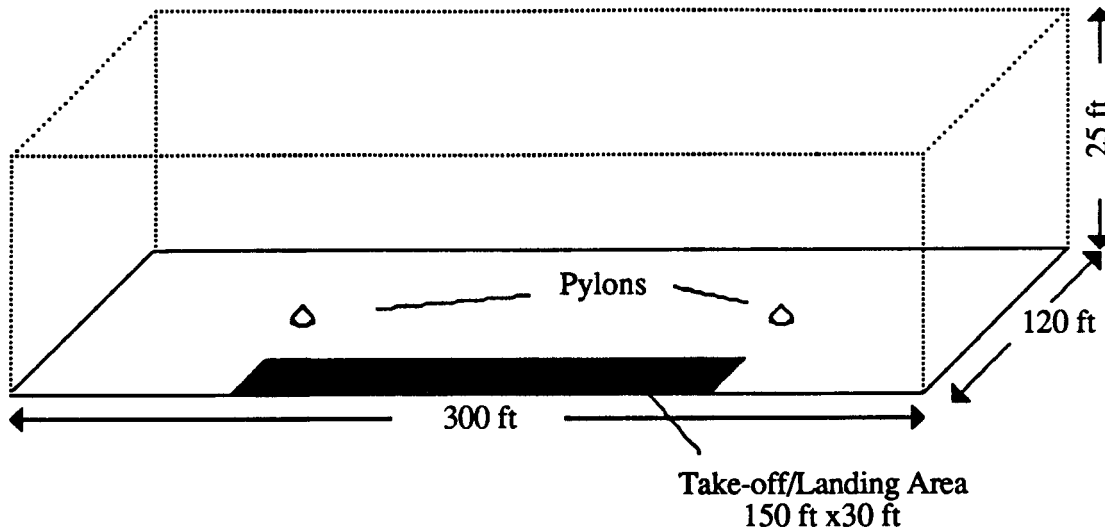
### 7.1 Take-off Performance

Referring to Fig. 7.1.1, recall that the mission objective concerning take-off is to reach take-off speed and lift off from the ground in a distance of 75 ft, followed by ascent to cruise altitude (20 ft) within another 75 ft. Based primarily upon the argument that the power required to take-off within these prescribed limits and climb to the proper altitude is much greater than the power needed for the remainder of the mission (i.e. steady, level flight and simple maneuvers), it has been decided that a catapult-type launch should be implemented into the design. By doing so the general size of the propeller motor need not be oversized for take-off, thereby reducing total plane weight both directly and indirectly - a smaller amount of battery power will be needed to power the smaller motor, hence a reduction in battery weight.

As should be evident from the preceding introduction, the airplane will rely on a conversion of kinetic energy (in the form of a high initial take-off speed) into potential energy in order to assist the on-board propulsion system in bringing the airplane to its proper cruise altitude. This procedure will be referred to as a "zoom take-off." In order to estimate the take-off speed necessary to meet the mission requirements, a simple computer routine was developed which essentially performed a numerical integration of Newton's Second Law. The rationale for doing so is fully explained in Appendix B, and the reader should consult this section for a complete explanation. Suffice it here to say that the method effectively steps the

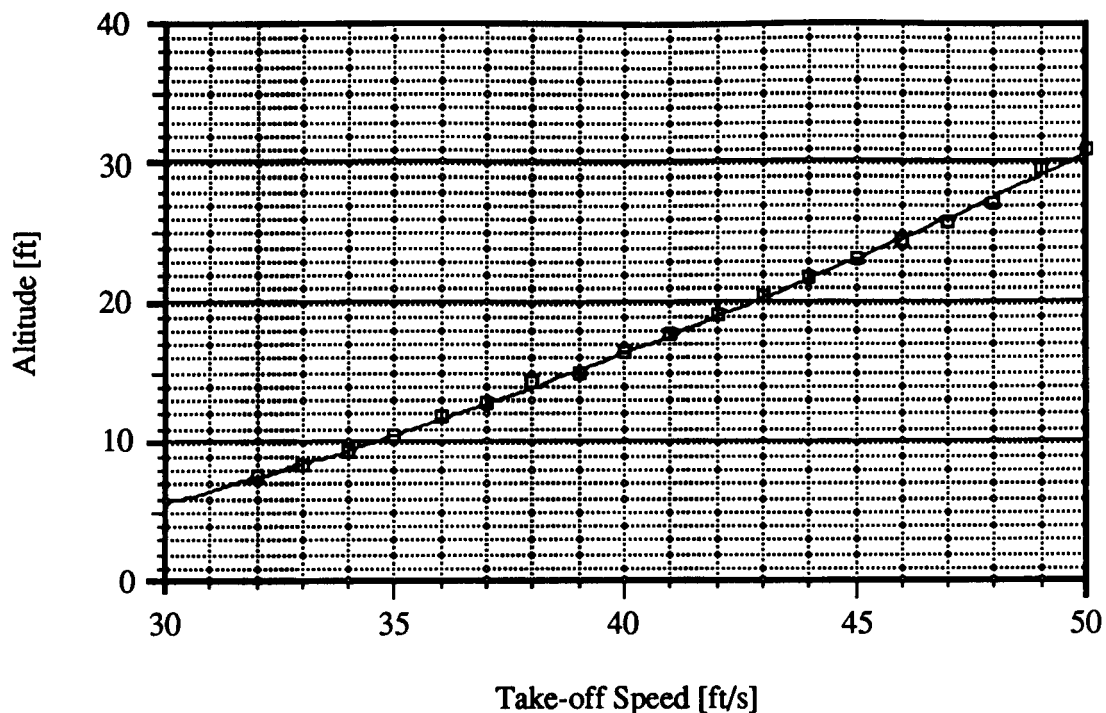
motion of the plane through differential time elements at which point the external forces exerted on the plane are calculated and used to update the velocity and position vectors.

**FIGURE 7.1.1** Three-dimensional View of Closed Course



The results of the take-off analysis based on present airplane designs are presented in Fig. 7.1.2. Notice that a take-off speed of 42 ft/s would theoretically bring the plane to its exact cruise altitude of 20 ft. However, since higher speeds are most likely accompanied by more severe load factors and hence greater structural requirements, it has been decided that a target take-off speed of 35 ft/s be selected. This will assist the plane by bringing it to approximately 3/4 of its cruise altitude. The remaining 5 ft should be easily attained in the remaining take-off distance by the power of the propeller alone. In an effort to verify these results, a simple kinetic/potential energy balance was performed (see section B.4 of Appendix B). Judging from these calculations, it appears that the computer routine is working correctly. However, it should be noted that an exact solution isn't expected or even needed. The only reason for developing the computer routine was to provide some "ball-park" figures for required take-off speed. In this regard the method of analysis has worked quite nicely.

**FIGURE 7.1.2** Theoretical Altitude Reached Upon Attainment of Cruise Velocity as a Function of Take-off Speed



In order to accelerate the plane to this take-off speed, a small independently controlled take-off cart has been designed (see Fig. 7.1.3) The cart is a four-wheeled vehicle (two axles) which is powered by a geared belt drive/electric motor combination. Aside from the motor, speed controller and battery pack, the cart consists simply of a swivel bar upon which the plane will rest by means of a small notch running cross-wise through the bottom of its fuselage (see Fig. 7.1.4). In order to keep the plane from lifting off the cart before take-off speed is reached, the plane will be inclined at a slightly negative angle of attack, and the notch will be positioned just behind the airplane's center of mass. Note that the landing gear is used to support the plane at the proper angle. After the cart has accelerated the plane to a speed of 35 ft/s, the pilot will gently rotate the airplane by deflecting the canard, at which time the plane should lift off the cart altogether and begin its climb. [Original designs had the cart physically constraining the plane at some prescribed positive lift angle until take-off speed was reached. However, upon further discussion, it became apparent that the plane would most likely not be

in a trimmed position upon release and would therefore be extremely difficult, if not virtually impossible, to control. The present scheme of allowing the plane to rest on the bar and gradually rotate to a positive lift angle is a direct result of this dilemma.] Present designs have the cart controlled simply by a guide wire running the length of the take-off area, with on/off control provided by a “rip cord” connected to a removable fuse at the rear of the cart. However, a spare remote-control unit could be implemented in order to provide steering and throttle control should it be deemed necessary.

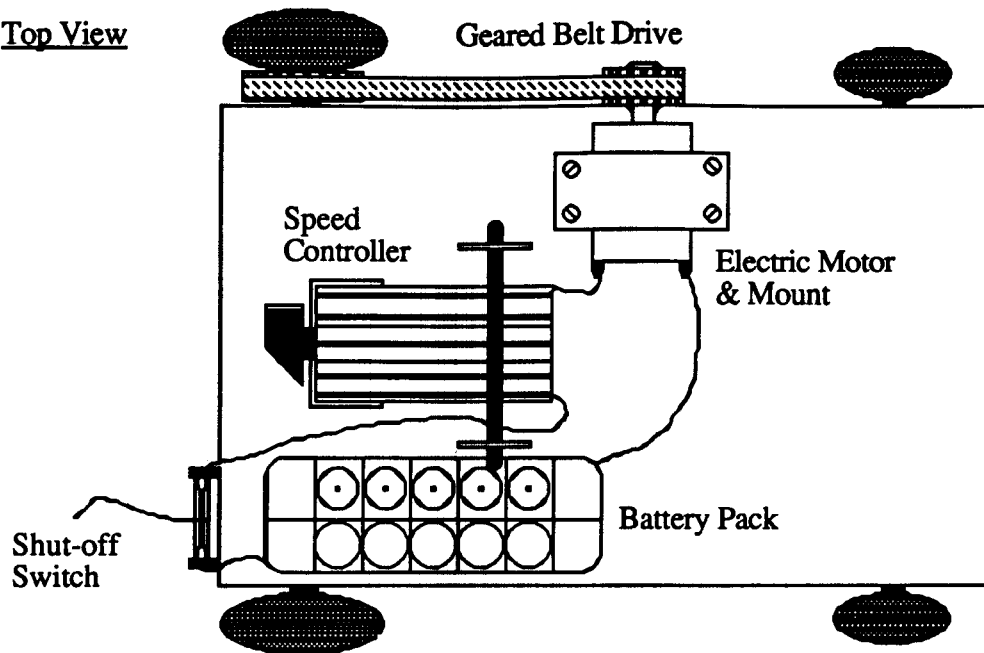
Prior to the actual flight of the airplane, we hope to be able to test the performance of the cart and determine if the plane will indeed be able to rotate about the pivot bar upon reaching take-off speed (35 ft/s). The airplane itself is essentially a tail dragger with adjustable front landing gear. It was designed in this manner specifically to allow the plane to be realigned on the cart at a new attack angle should the situation arise. We are confident that after one or two tests a satisfactory alignment will be found, and if the plane remains stable immediately upon lift-off, it will have a good chance of meeting its take-off requirements.

Once again, the sole purpose for utilizing a take-off cart is to lower the net weight of the airplane by reducing the size and weight of the propulsion system. Utilizing a take-off cart is essentially the same as “hand launching” the plane. However, because the plane itself will have so little excess power, it is necessary to accelerate it to a relatively high velocity so that it gains enough kinetic energy to “zoom” to cruise altitude. One would have to be an extremely fast runner to produce the same effect with a “hand launch”. Furthermore, the odds of the plane being in a trim position upon release seem much lower for the “hand launch” than for the take-off cart.

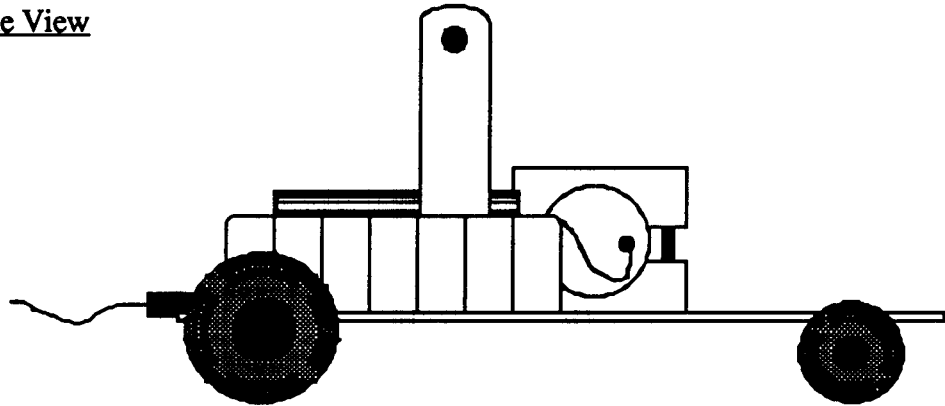


**FIGURE 7.1.3** Three-View Scaled Drawing of Take-off Cart (scale 1:4)

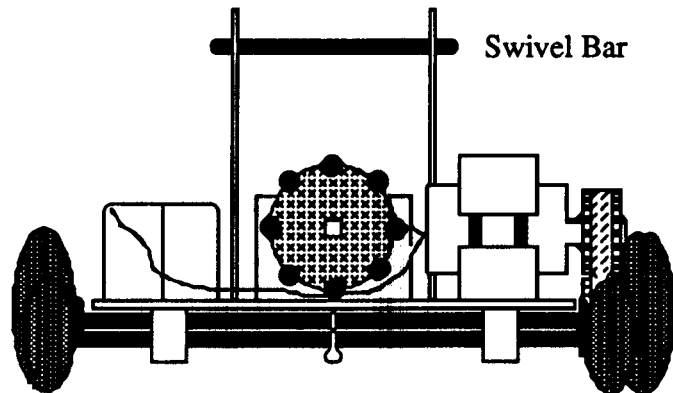
Top View



Side View



Front View



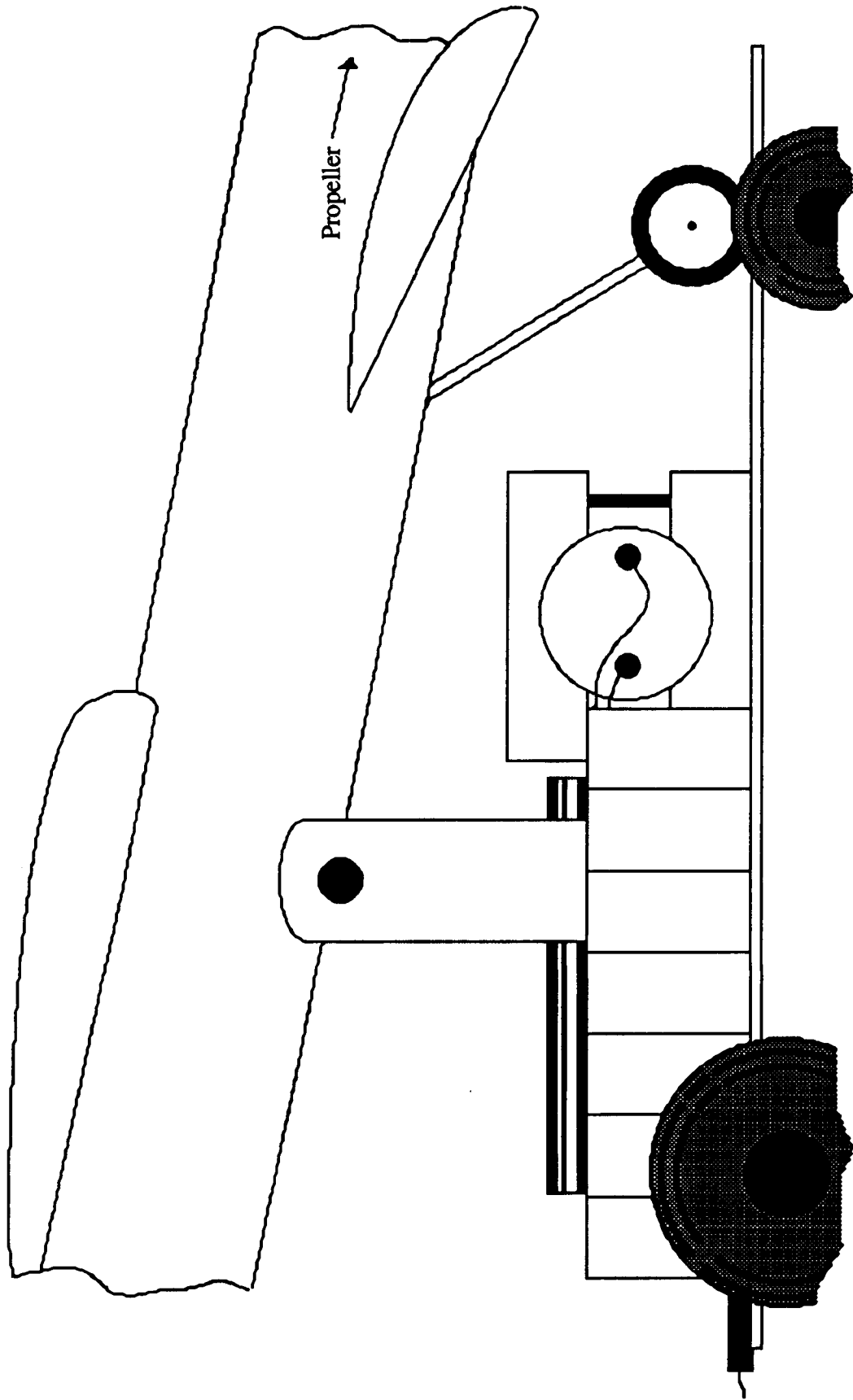


**FIGURE 7.1.4** Side View of Cart with Partial View of Plane Resting in Proper Take-off Attitude

## **7.2 Range and Endurance**

Assuming that the powered cart successfully launches the Dawdler up to the design altitude, the on-board propulsion system will not have to draw any extra current for this part of the flight. The rest of the mission consists of straight level cruise and banked level turns. It has been predicted that the current drain from the battery will be approximately 9.3 A during the level cruise sections. Because the pilot will be pulling back on the stick to maintain level flight during the turns, he will also have to increase the motor speed slightly to maintain cruise velocity. The current drain will therefore be slightly higher during the turning maneuvers. It is estimated that the current drain during the turns will be 9.7 A.

The propulsion system will use 500 mah batteries, giving the design an estimated endurance of 190 seconds. This assumes that the flight consists of equal times of level flight and turning flight. This endurance is also the maximum endurance, because the current drain is a minimum at the cruise velocity. The range corresponding to the maximum endurance at  $V=25$  ft/s is approximately 4750 feet. The maximum range for the aircraft design occurs at a slightly higher velocity of  $V=30$  ft/s and is approximately 5290 feet. The endurance at this flight speed is about 175 seconds.

## **7.3 Power Required and Available**

The power required and several power available curves are given in Fig. 7.3.1. It is seen that the minimum power required for the Dawdler design occurs at a velocity of about 20 ft/s. For velocities less than this the induced drag begins to dominate, while for velocities higher than 20 ft/s the skin friction drag increases.

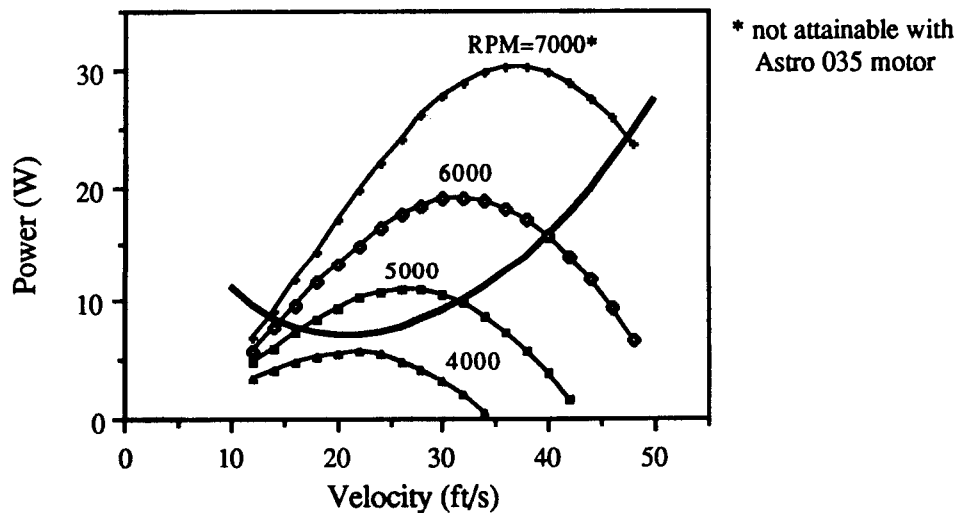
To maintain level flight at the cruise velocity of 25 ft/s, the propeller speed must be approximately 4450 rpm. By increasing the propeller speed, the aircraft can either cruise at a higher velocity or climb. The engine is limited to a maximum propeller speed of about 6200 rpm with the chosen applied voltage of 6.75 volts. At this maximum motor speed, the current

in the armature is estimated to be no higher than 16.5 amperes but no lower than 14 amperes. Thus, even if a higher voltage were applied, the maximum current the system could withstand would soon be reached.

The maximum power available is about 20 watts at a velocity of 32 ft/s and 6200 rpm. The maximum excess power ( $P_{av}-P_{req}$ ) available for climbing occurs at a slightly lower velocity of 29 ft/s. This means that the Dawdler has its maximum rate of climb capability when flown at 29 ft/s.

The maximum speed the Dawdler can attain is estimated to be around 40 ft/s. This is where the maximum power curve intersects the Dawdler's  $P_{req}$  curve. The minimum velocity that the RPV can fly at and remain aloft is 14 ft/s as seen in Fig. 7.3.1. However, because of the low Reynolds numbers, it is believed that the wing will stall at 17.5 ft/s.

**FIGURE 7.3.1** Power Available for Master Airscrew 9-6



#### 7.4 Climbing and Gliding Performance

As mentioned above, the maximum excess power occurs at a velocity of 29 ft/s. At this velocity, the maximum rate of climb, given by  $R/C=(P_{av}-P_{req})/W$ , is estimated to be 3.2 ft/s.

Note that if the Dawdler's weight,  $W$ , increases the R/C will diminish considerably. The R/C at cruise velocity is estimated to be 2.7 ft/s. The Dawdler should be able to climb over 18 feet during one of the mission's 175 ft straightaways. This is more than adequate since the turns will be made at a fairly level altitude and the take-off is assisted by an externally powered cart.

The gliding performance can be characterized by two figures of merit, the minimum glide angle and the minimum rate of descent. The relations for these two parameters are given below:

$$\gamma_{\min} = \arctan(1/(L/D)_{\max})$$

$$(R/D)_{\min} = (2W/S)^{1/2}(C_D/C_L^{3/2})_{\min}$$

Given the design's maximum L/D of 11.5, the minimum glide angle for the Dawdler design is 50°. From this it is predicted that the maximum distance the Dawdler can glide from the 20 ft design altitude is 230 feet. Therefore, the Dawdler should be able to glide through the final turn and almost the length of the runway if it were to cut the motor. Consequently, if it is desired to keep the airplane aloft as long as possible, the minimum rate of descent is approximately 2.1 ft/s, and the Dawdler could glide for almost 9.5 seconds. A summary of the Dawdler's performance is given in Table 7.4.1.

**TABLE 7.4.1** Summary of Performance Predictions

$W = 2.3 \text{ lb}$	Batt. Cap. = 500 mah
$S_w = 3.24 \text{ ft}^2$	$S_c = 1.4 \text{ ft}^2$
Max flight speed = 40 ft/s	
Max rate of climb = 3.2 ft/s	
Wing loading, $W/S_w = 11.4 \text{ oz/ft}^2$	$(W/S_{\text{tot}} = 8 \text{ oz/ft}^2)$
Max endurance = 193 s	
Range at max Endurance = 4750 ft	
Max Range = 5290 ft	
Min glide angle, $\gamma_{\min} = 5^\circ$	
Min rate of sink, $R/D_{\min} = 2.1 \text{ ft/s}$	

## **VIII**

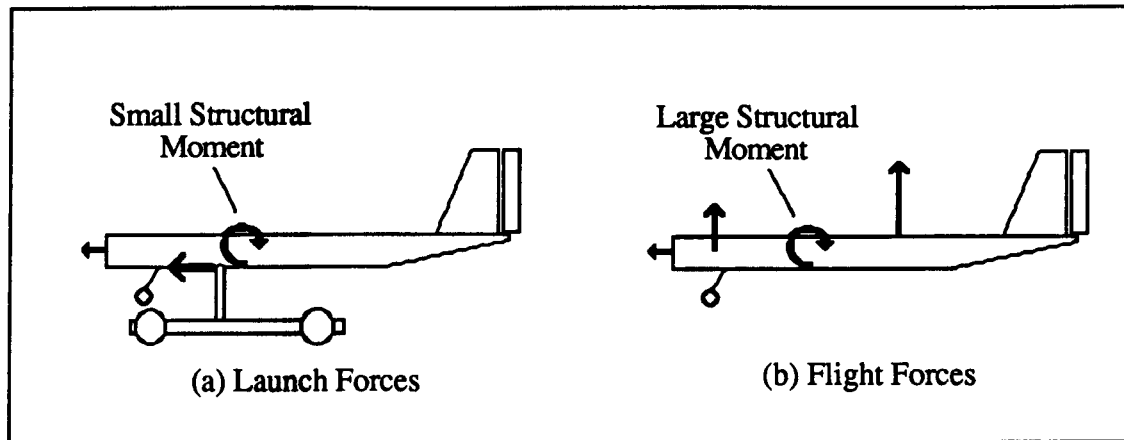
# **Structural Design**

### **8.1 Flight and Ground Load Estimation**

For this aircraft, there are not going to be significant ground loads. In our particular type of launch, the vehicle will see a significant force during the first few seconds of take-off roll, but not much after. The surface on which the take-off occurs is very smooth and should not provide any significant bumps to jar the aircraft. Since the largest horizontal force during take-off occurs along the length of the fuselage, the largest bending moment applied to the fuselage is not significant. See Fig. 8.1.1(a). During the rotation phase of the takeoff, however, the fuselage does sustain a large bending moment located near the leading edge of the main wing. This is due to the exceptionally large forces that may be created by the lifting surfaces at take-off speed. See Fig. 8.1.1(b). In order to sustain these loads, the cross sectional area of the main balsa wood beams running the length of the fuselage have been sized at 0.25" x 0.25" square. Selection of the take-off pivot point near the center of gravity of the aircraft has eliminated the static bending moments at the beginning of the roll. For landing, the aircraft is equipped with two, lightweight landing gear wheels located at the front of the aircraft. These are here for the sole purpose of preventing the propeller from contacting the ground on landing. Due to the weight requirements which we have placed on our aircraft, the landing gear is not able to sustain very large impact loads. Our maximum wheel diameter was set at 1.5" and preliminary estimates show that the balsa wood struts should be 6" long. It is expected that

upon landing, the pilot will be able to maintain a relatively slow rate of descent to prevent breaking of the landing gear.

**FIGURE 8.1.1** Ground and Flight Load Diagram



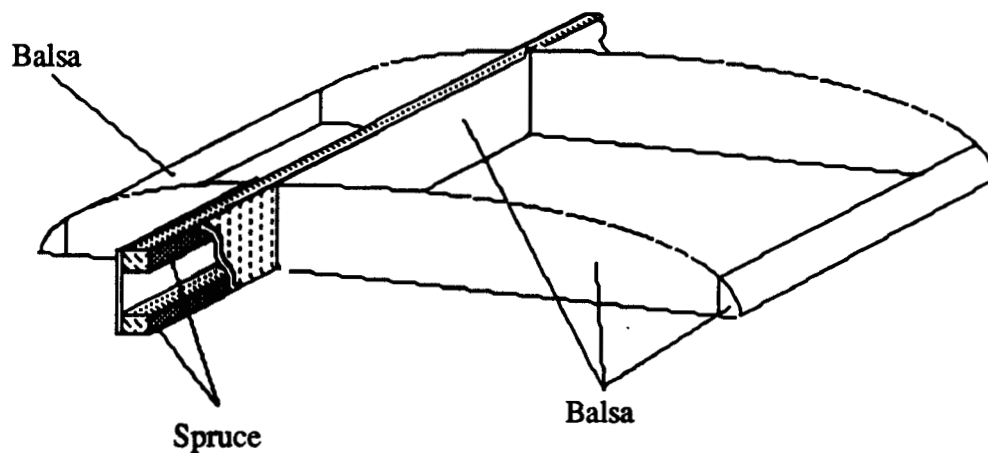
## 8.2 Structural Components

The main structures involved in this aircraft are the wing, canard, fuselage, and vertical stabilizer. The first of these components is the wing. For our aircraft, weight is the most important factor. Therefore, a lightweight wing is a necessity. The effects of various main spar configurations were examined to determine the strongest strength spar with minimum weight. Rectangular wing spars, circular spars, and triangular spars were examined. The results of analysis concluded that the main spar should be made of spruce caps with non-structural balsa supports. This allowed for lightweight construction and minimum deflection under the largest load. Preliminary design estimates show that the cross section of the main spar caps should be 1/4" wide by 3/16" tall. Balsa leading and trailing edge spars were used to sustain any horizontal loads which were expected to be minimal. A special feature of the main wing is the removable wingtips. The requirement for our wing to fit into a given volume was violated by the 5 ft wing span. This necessitated the use of 1/2 ft, separable wing tips. Connection of the wing tips to the main section was accomplished by a rectangular connector

which fits between the spar caps. Loads on the wingtips are not significantly high so that a spruce connector should adequately support the load.

The canard was constructed in a similar manner with the exception of the use of a circular dowel at the root. This would allow for the entire canard to pivot. Preliminary estimates show that a wood dowel with a diameter of 5/16" should be able to sustain the vertical loads, however, the ability to sustain the torsional load with minimum twisting is unknown at this point. A fully moving canard was selected so that it may provide a wide range of loads without complicated control mechanisms. Both the wing and the canard will be covered in Monokote to provide shape and torsional stability. See Fig. 8.2.1 for the structural layout of the wings and canard.

**FIGURE 8.2.1** Wing and Canard Construction



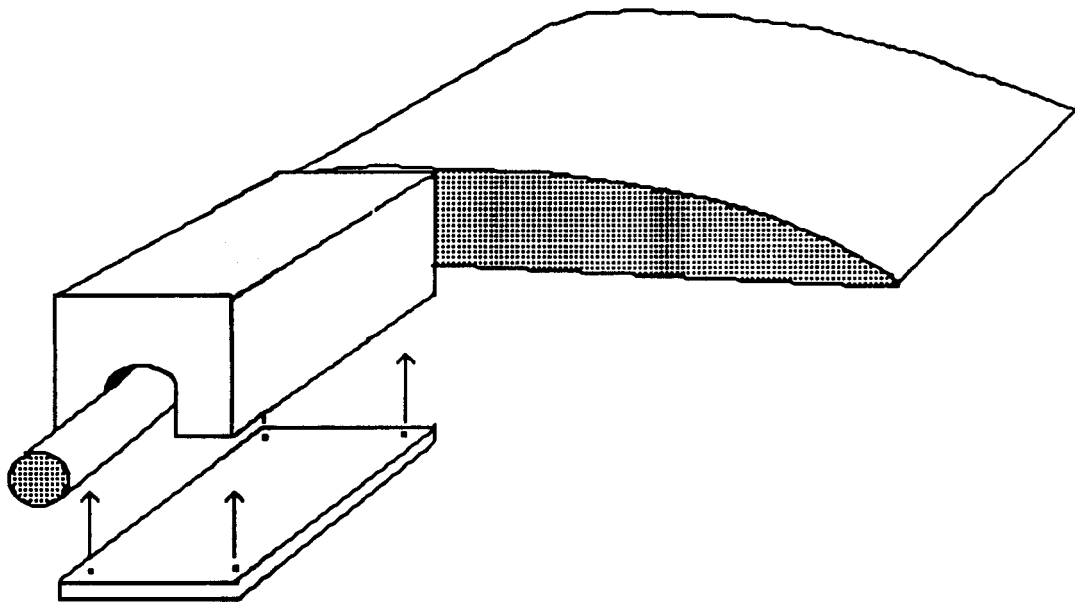
The third structural element is the fuselage. The construction is of a box frame type composed entirely of balsa. Thin balsa planking is placed on the outer surface to give additional support without increasing the weight dramatically. The omission of this outer skin was examined, but it was decided that the extra support given to the main frame was significant enough to warrant the weight penalty.



The final element is the vertical stabilizer. This is mainly a flat plate constructed of a main spar, leading edge spar and trailing edge spar. Several small ribs are spaced vertically to give the stabilizer support. The trailing edge must be quite strong since a rudder is connected to it. The vertical tail will also be covered in Monokote. While this is a large portion of the fuselage weight, it is a necessary one. Due to the need for a rearward center of gravity, the relatively heavy tail aids in achieving this.

The fuselage and vertical stabilizer will be a complete unit. The wing and canard will each be an independent piece. Due to the storage requirements, it is necessary that the canard and the wing be removable. The canard will be detached by removing a mounting plate located on the underside of the fuselage. See Fig. 8.2.2. The wing will be connected to the fuselage by the use of rubber bands. Access to the control systems will be achieved through an access hole below the main wing. As most of the equipment is located in the rear, access should not be a significant problem.

**FIGURE 8.2.2** Canard Mounting Mechanism



### **8.3 Material Selection**

Because of the nature of our design, the weight was considered the main objective in the design of the aircraft. In accordance with this objective, we needed to select materials which would be strong enough but remain light enough to assemble the RPV in the allotted weight range. Many types of materials were available for the construction of the aircraft. These included fiberglass, plastics, wood and composites. Of these, woods and composites were the only materials that were light enough. Of the types of woods, only spruce and balsa were considered. The reason for this was that balsa was a relatively strong material, strong enough for the loads seen during flight, and that spruce was significantly stronger than balsa but was also relatively light. Spruce was used only in one place, that being the wing and canard spar caps. Balsa was used on all of the rest of the aircraft since no major loads were expected in these areas. Composites were examined for a short time. Their significant strength advantage and relatively light weight made it a candidate. However, due to the cost of the composite material (carbon fiber) and the complexity of construction, this material was discarded. The ease of construction and availability of balsa wood and spruce along with the relatively low cost made the material selection quite easy.

# **IX**

## **Technology Demonstrator**

A full scale technology demonstrator was constructed to test the feasibility and air-worthiness of the Dawdler design. The following sections will highlight the resulting configuration, construction, and cost details as well as the flight test results.

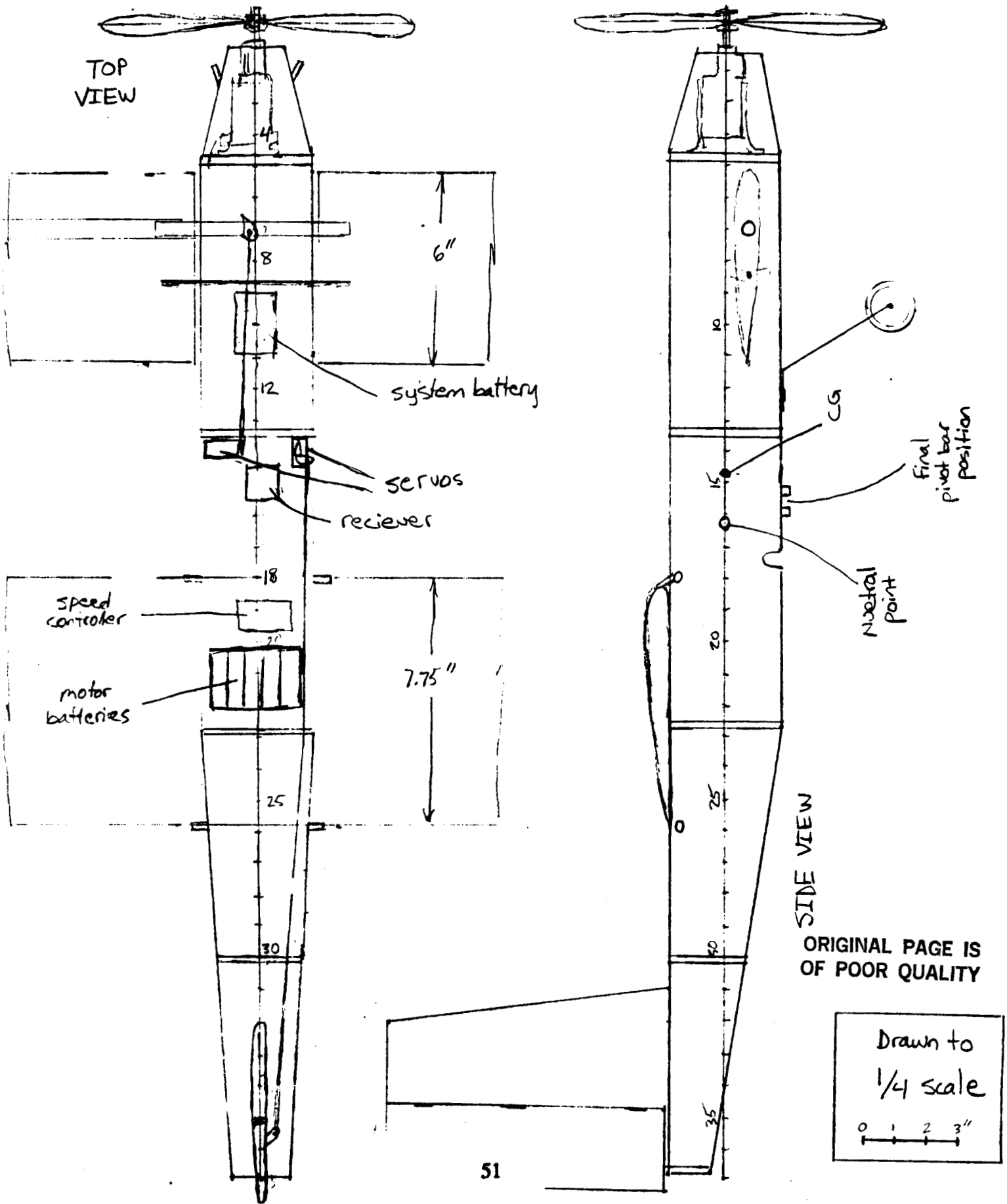
### **9.1 Configurational Data and Geometry**

#### **9.1.1 Airplane**

The overall appearance and configuration of the tech demo did not vary much from the final preliminary design. Small changes were made in the following areas:

- The vertical tail was moved aft an extra 1.0 in.
- The canard was made in two pieces that attached to a permanently mounted rod in the fuselage. It was originally desired to have a single piece canard that could be removed from the bottom floor of the fuselage.
- The wing was mounted at 0° angle of attack with respect to the fuselage reference line instead of the 4.35° planned on in the design. This was done as a suggestion from an experienced model aircraft pilot in order to trim the wing better during the take-off.
- The main landing gear were moved aft 3.0 in to avoid obstruction of the deflection of the canard.
- A 10 in propeller was used instead of 9 in.

**FIGURE 9.1.1** Internal Configuration of the Technology Demonstrator



- The final pivot bar joint had to be moved 1.5 in closer to the cg to decrease the moment required for take-off rotation.

Figure 9.1.1 shows the final configuration of the essential components of the technology demonstrator.

### **9.1.2 Launch Cart**

The launch cart underwent many significant changes during its development and testing. Originally, it was planned to make it a “turn-it-on-and-let-it-go” type system, but it turned out being fully controllable, thanks to available equipment and the help of both an electrical and a mechanical technician. The cart was powered by a separate Astro 15 motor which turned the rear axle by means of cogged gears and a notched belt. A gear reduction of 2:1 was used. The motor required 16 volts to turn the 3.25 in wheels at the 2500 rpm necessary to reach the desired 30-35 ft/s.

## **9.2 Weights**

The technology demonstrator had a take-off weight of 2.7 lb. This was 17% heavier than the design weight of 2.3 lb. A weight breakdown is given in Table 9.2.1. The most surprising fact was that no trouble was encountered in locating the cg as aft as desired. In fact, the compartment originally designed to hold the motor batteries and speed controller was not even used. Instead, these items had to be placed under the wing to move the cg forward. The cg was placed 1.47 inches in front of the neutral point for a static margin of 19% MAC. Because no trouble was encountered in keeping the cg aft, it is possible that the fuselage could be designed shorter allowing a slightly lighter design. However, the vertical tail might also have to be made larger to counter the shorter moment arm.

**Table 9.2.1 Summary of Weights of the Technology Demonstrator**

	<u>target values</u>	<u>actual values</u>
total T.O. weight	2.3 lb	2.7 lb
wing area	3.24 ft <sup>2</sup>	3.24 ft <sup>2</sup>
wing loading	11.4 oz/ft <sup>2</sup>	13.3 oz.ft <sup>2</sup>
<u>Wing:</u>		
4 foot midsection	—	6.07 oz
2-6 inch wing tips	—	2.11 oz
entire wing	8 oz	8.18 oz
		<hr/> WF = 19%
<u>Canard:</u>	—	3.6 oz
<u>Vertical Tail:</u>	—	N.A.
<u>Propulsion System:</u>		
Astro 035 motor	5.5 oz	6.9 oz
battery pack (5 x 500 mah)	3.9 oz	4.3 oz
motor mount	—	1.29 oz
speed controller	3.0 oz	1.25 oz
total weight	12.0 oz	14.24 oz
		<hr/> WF = 34%
<u>Control System:</u>		
2 servos	1.2 oz	1.31 oz
receiver	0.95 oz	0.95 oz
batteries (4 x 250 mah)	2.0 oz	2.1 oz
linkages	—	N.A.
<u>Landing Gear:</u>		
	1.8 oz	~1.0 oz
		<hr/> WF = 2%
<u>Fuselage:</u>		
(with vertical tail)	9.0 oz	11.4 oz
		<hr/> WF = 55%

### 9.3 Manufacturing and Cost Details

The entire airplane was constructed primarily of balsa, spruce, plywood, and Super Monokote. Spruce was used in the wing spars and fuselage longerons to provide the desired stiffness. Thin 1/16" plywood sheeting was used for surfaces that would experience impacts and heavy loads such as the tail bottom (which would drag on landing) and the firewall to which the motor mount was connected. Layering the plywood over balsa provided a light and durable material.

**Other details of interest:**

- The Monokote may have contributed up to 2.2 oz of the total wing weight.
- Monokote was applied over the 1/16" thick balsa sheet fuselage walls. Although it was aesthetically pleasing, it may have contributed unnecessary weight.
- All of the top panels of the fuselage were attached with small screws to allow easy access to all interior regions.
- Velcro was used to secure batteries, receiver, speed controller, and even the engine cowling. It was quite handy.
- Wing box spars, although made with only two 1/8" x 1/8" spruce beams and 1/16" thick balsa sheeting, exceeded our expectations for strength and stiffness.

The launch cart was constructed out of scrap wood and aluminum, an unused Astro 15 electric motor, and some leftover batteries. Wooden dowels were originally used for the axles, and some spare gears and a notched belt were used as a transmission system. Practically everything except for the wheels was free, being on-hand supplies from the Aerospace Engineering Department. The launch cart could, however, become quite a financial burden if the equipment were not already on hand.

Although the cart was originally designed to just be turned on and let go, guided only by a taut string attached to a padded weight at the end of the take-off strip, the performance proved to be unacceptable. A "kill switch" made of a fuse pulled out by a string, was added to eliminate the destructive impacts (the cart kept breaking). The cart also did not steer well. The guide string merely stretched when the cart veered left or right, instead of keeping it straight.

A decision could have been made to simply use a metal wire instead of string for guidance, but the cart also had the problem of large acceleration rates. The cart accelerated at up to 25 ft/s<sup>2</sup> (0.8g's) immediately after release. It was feared that this might throw the Dawdler and cause serious damage to its lightweight structure. To eliminate both the steering

July 24, 1990:

Pages 55 and 56 removed because of  
funding information-

  
PHILIP N. FRENCH  
Document Evaluator

54A



Extensive testing was done on the launch cart before the RPV was ever placed on it. Evaluations had to be made of the steering, speed, and acceleration.

#### First Tests

- Cart steered poorly even with guide string
- 15 yd timings were made to estimate speed at several voltage settings.
- Front axle support broke on 3rd impact with cushioned weight — kill switch was added.

#### Second Tests

- Directional tests performed poorly again after changes made to front axle direction.
- Cart was found capable of reaching speeds of 32 ft/s.

#### Third Tests

- Wood drive axle snapped under torque loading (replaced with steel axle).
- Discovered directional problems were related to the directional grain of the artificial turf, not the steering system.
- Large acceleration rate considered unacceptable. Decision made to employ fully controllable cart.

### 9.5.2 Aircraft

#### Taxi test

- As designed, the Dawdler did not have enough stand-alone power to reach take-off speed. Proper tests were delayed while cart changes were being made.

#### Take-off test

- Plane remained quite stable on the launch cart pivot bar, but canard could not provide enough lift to rotate the craft for lift-off.
- Pivot bar height was adjusted, but eventually the pivot position had to be moved closer to the cg.

- Canard control neutral position was adjusted, and the wing was remounted at 0° incidence by suggestion.

#### Flight test

##### 1st run

- Pilot had difficulty keeping plane on cart due to not enough negative angle of attack of the canard and wing. The RPV left the cart early, did not have enough power to climb, and stalled, breaking the propeller upon impact with the ground. The fully moveable canard appeared to be quite sensitive to pilot input so the amount of control throw was reduced.

##### 2nd run

- Pivot bar was raised 1.0 inch to decrease the angle of attack during ground roll. The plane rotated well and lifted off but did not gain enough altitude. The inside wing stalled during the first turn and the plane landed roughly.

##### 3rd run

- Pilot kept plane on cart until it reached a velocity of 31 ft/s. The plane zoomed up to an altitude of about 15 feet. After several quick oscillations, the pilot recovered and trimmed the plane quite successfully. The plane completed one very smooth and slow “figure 8” lap before running out of battery energy and landed smoothly.

The flight speed was estimated from stop watch timings at 21 - 25 ft/s. The technology demonstrator appeared to have good handling qualities, but almost no rate of climb capability. This could have been due to either a slightly lower battery voltage caused by the drain of the first two attempts or the fact that the technology demonstrator was 6 oz over the design take-off weight. The range and endurance were significantly less than predicted, approximately 290 yds and 40 seconds respectively, but overall the aircraft performed almost exactly as desired.

## 9.6 Recommendations

- 1) The fully maneuverable canard of relatively large size (40% of the wing area) appears to be quite sensitive to pilot input. Control deflections should be kept small, or alternatively elevators (moveable flaps) could be used. However, a fully moveable control surface can be quite forgiving with uncertainties in setting the incidence angles. We completely readjusted our wing incidence angle but only had to adjust the servomotor angle of the canard to retrim the aircraft.
- 2) The propulsion system appeared to have just enough power to cruise at a speed of 21 - 25 ft/s and had almost no rate of climb capability. This is most likely because the technology demonstrator was 6 ounces (17%) heavier than the target value of 2.3 lbs. However, the power output of the motor might still have been less than predicted. Very conservative estimates should be made for the propeller efficiency and motor power during initial design stages. It is recommended that the Dawdler be fitted with a slightly larger engine (e.g. an Astro 05 motor).
- 3) The powered cart proved to be a very feasible and practical tool in assisting the aircraft's take-off (once the bugs were worked out). The cart accelerated much faster than most of the other unassisted RPV designs, saved valuable on-board battery energy, and actually appeared to provide the Dawdler with better lateral stability during ground roll than other with designs with conventional fuselage-mounted landing gear.

It is recommended that this type of take-off cart be used only if it is fully controllable with respect to its velocity and steering. Too many problems arise with a "turn-it-on-and-let-it-go" type system. Having a separate person controlling the cart also appeared to be a good idea; it relieved the pilot of extra duties so that he could focus more closely on the performance of the aircraft.

The success of the mission with this type of launch, however, depends heavily on the pilot being able to trim the aircraft in the moments after lifting off the pivot bar.

Also note that the cost of the this type of system can be prohibitive unless the control equipment is already available.

## X

### **Extension of Mission to High Altitude Long Duration Station Keeping Mission**

A great deal of interest has been shown in developing a remotely piloted vehicle that can keep a relatively constant station at a very high altitude. These types of missions are often called high altitude aircraft platforms, or simply HAAP's. The ultimate goal would be to develop a system that could keep an HAAP at a high altitude station indefinitely, without ever having to refuel it. Such a design could be used for such applications as wide ranging as forest fire detection, marine mapping and observation, communications broadcasting, or atmospheric or astrophysics (radiation) monitoring.

This type of long duration mission would require a special propulsion system. A direct application of the Dawdler design would require 6 hours to climb to 70,000 ft and an enormous battery capacity of 80,000-100,000 mah! This would mean batteries that would weigh over 45 lb, and that is just to climb to the platform. A great deal more battery capacity would be required to maintain this platform for a reasonable amount of time. A study by E.B. Graves has indicated three special types of propulsion systems receiving the most attention.[8] These are solar-voltaic cells, ground based microwave beams, and nuclear propulsion systems. It was determined that refueling or rotation methods would be uneconomical.

The ground based microwave systems were found to be the most feasible of the three. This type of system would rectify a microwave beam sent from the ground and convert the energy into electricity to drive a propeller. Solar power systems were found to require large

surface areas to produce useful quantities of electricity and would have to have heavy batteries to store electricity for nighttime hours. A design was proposed that would use solar energy to climb during the day and glide at night, but the altitude loss at night would be excessive. Finally it was determined that society would object to nuclear powered HAAP's.

In general it was found that airplane type designs were not as feasible as blimp type designs. The main reason for this is that airplanes require dynamic lift to stay aloft. At high altitudes, the density of air is greatly reduced, meaning the aircraft has to have much larger lifting areas or fly at higher velocities. It is generally agreed upon that a HAAP would have to be stationed at an altitude of at least 70,000 ft because at lower altitudes high atmospheric wind speeds or jet streams would be a serious design concern.

Overall, the view is pessimistic in ever being able to design an airplane type HAAP such as the Dawdler with current levels of technology. It is estimated that a solar powered HAAP would require lift coefficients of up to 1.5 at  $Re$  between 0.1 and 0.3 million due to the heavy weight of the lengthy wings and storage batteries. Relatively few airfoils have been designed that can provide this high of  $C_L$  at those low values of Reynolds numbers. Further, it appears that HAAP's would be more expensive and less flexible than aircraft that are currently performing high altitude missions.

Key technological needs necessary to develop a successful airplane type HAAP include reducing the weight of rechargeable batteries, developing strong and very light weight structural materials, and developing airfoil sections that can high lift coefficients at low Reynolds numbers. Further, either an economical method of beaming and rectifying microwaves would have to be developed, or considerably lighter solar cells developed for a solar powered system. Unless these needs can be met, the future is bleak for airplane type HAAP's implementing solar power.

## References

1. AstroFlight Inc., 1331 Beach Ave. Marina Del Rey, CA 09292.
2. Department of Aerospace & Mechanical Engineering, University of Notre Dame, Spring 1990.
3. Young, B.N., "Propeller Performance Analysis for Small Computers," Masters Thesis, University of Notre Dame, May 1984.
4. Roskam, Dr. J., *Airplane Design, Part II: Preliminary Configuration Design and Integration of the Propulsion System*, Roskam Engineering and Aviation Corp., Ottawa, KS, 1985.
5. Beron-Rawdon, Blaine, *Model Aviation*, 'Dihedral: Part 3,' October 1988.
6. Lennon, A.G., *RIC Model Airplane Design*, 1986.
7. Nelson, R.C., *Flight Stability and Automatic Control*, 1989.
8. Graves, E.B., "The Feasibility of a High-Altitude Aircraft Platform with Consideration of Technological and Societal Constraints," NASA Technical Memo 84508, June 1982.
9. Nicoli, Leland, *Fundamentals of Aircraft Design*, 1975.
10. Riegels, Friedrich, *Airfoil Sections*, 1961.

---

**APPENDIX  
A**

---

**STABILITY DERIVATIVE ESTIMATES**



## A.1 Lateral

$$C_{l\beta} = (C_{l\beta})_{\text{wing}} + (C_{l\beta})_{\text{canard}} + (C_{l\beta})_{\text{vert stab}} + (C_{l\beta})_{\text{wing-fuse}} + (C_{l\beta})_{\text{can-fuse}}$$

$$(C_{l\beta})_{\text{wing/can}} = (C_{l\beta})_{\Gamma} + (C_{l\beta})_{\text{basic sweep}}$$

$$(C_{l\beta})_{\Gamma} = -0.25C_{L\alpha}\Gamma\left[\frac{2}{3}\frac{1+2\lambda}{1+\lambda}\right]$$

$(C_{l\beta})_{\text{basic sweep}}$  from Fig. 21.9 Leland

$$(C_{l\beta})_{\text{w-f/c-f}} \sim \begin{array}{ll} -0.344 / \text{rad} & \text{high} \\ 0.0 / \text{rad} & \text{mid} \\ +0.0458 / \text{rad} & \text{low} \end{array}$$

$$(C_{l\beta})_{\text{vert stab}} = -(C_{L\alpha})\left(1 + \frac{\partial\sigma}{\partial\beta}\right) \frac{q_{vs}}{q} \frac{S_{vs}}{S} \frac{Z_{vs}}{b}$$

$$\left(1 + \frac{\partial\sigma}{\partial\beta}\right) \frac{q_{vs}}{q} = 0.724 + \frac{3.06S_{vs}/S_w}{1 + \cos\Lambda} + 0.4 \frac{Z_w}{d} + 0.009AR_{\text{wing}}$$

## A.2 Directional

$$C_{n\beta} = (C_{n\beta})_{\text{fuse}} + (C_{n\beta})_{\text{wing}} + (C_{n\beta})_{\text{canard}} + (C_{n\beta})_{\text{vert stab}}$$

$$(C_{n\beta})_{\text{fuse}} = -1.3 \frac{Vol}{S_{wb}} \frac{h}{W}$$

$$(C_{n\beta})_{\text{wing/canard}} = C_L^2 \left[ \frac{1}{4\pi AR} \right]$$

$$(C_{n\beta})_{\text{vert stab}} = \frac{l_{\text{vert stab}} S_{\text{vert stab}}}{S_{wb}} (C_{L\alpha})_{\text{vert stab}} \alpha_{\text{vert stab}}$$

$$(C_{L\alpha})_{\text{vert stab}} = \left( \frac{1}{2\pi n} + \frac{1}{\pi AR} \right)^{-1}$$

$$n=0.84 \quad Re=10^5$$

---

**APPENDIX  
B**

---

**ZOOM TAKE-OFF ANALYSIS**

## B.1 Mathematical Basis for Numerical Solution

Recall Newton's Second Law:

$$\Sigma F_x = m a_x = m (dV_x/dt)$$

$$\Sigma F_y = m a_y = m (dV_y/dt)$$

This can be approximated by introducing differential elements...

$$\Sigma F_x \approx m (\Delta V_x/\Delta t) \quad (1)$$

$$\Sigma F_y \approx m (\Delta V_y/\Delta t) \quad (2)$$

This basically assumes that the forces acting on the body remain constant over the differential time element  $\Delta t$ . In other words, given an initial set of conditions (i.e. position & velocity), the external forces ( $\Sigma F_x$  and  $\Sigma F_y$ ) can be calculated and thus the conditions at some differential time element  $\Delta t$  later can be determined by solving the above equation for  $\Delta V_x$  and  $\Delta V_y$ .

i.e.

$$V_{x,new} = V_{x,old} + \Delta V_x$$
$$V_{y,new} = V_{y,old} + \Delta V_y \quad \text{new velocities!}$$
$$\Delta X = (1/2)(V_{x,new} + V_{x,old}) \Delta t$$
$$\Delta Y = (1/2)(V_{y,new} + V_{y,old}) \Delta t$$

so

$$X_{new} = X_{old} + \Delta X$$
$$Y_{new} = Y_{old} + \Delta Y \quad \text{new distances!}$$

For the particular airplane in climbing flight, the main external forces will be the lift (of the wing and canard), the parasite drag of the entire plane, the induced drag (of the wing and canard), the weight of the entire plane, and the thrust of the propeller. Based on the specific airplane design and the instantaneous velocity, all of these forces can be calculated. Therefore, it would be quite easy to construct a simple computer routine which would utilize the above equations and effectively "step" through the climb by differential time elements  $\Delta t$ .

For example, immediately prior to take-off, the position and velocity of the plane are both known. From the design parameters and the velocity, the forces acting on the plane at that instant can be computed. Substituting the proper components into equations (1) & (2), the

differential change in velocity can be found at a differential time  $\Delta t$  later. This in turn determines the new velocity at time  $t_0 + \Delta t$ , and also the new position at time  $t_0 + \Delta t$ . The entire process is then repeated by using the new position and velocity to calculate the external forces.

## **B.2 Assumptions and Particular Design Values Used**

As introduced in section B.1, the approximate motion of the airplane upon take-off can be simulated by a relatively straight-forward numerical integration of Newton's Second Law. In order to provide realistic results, however, it is vital to model all the actual forces which will be acting on the airplane as accurately as possible. The following is a complete list of the actual design parameters used in the computer routine to determine the lift and drag forces acting on the airplane, along with the propeller thrust and the plane's net weight. Furthermore, the differential time element used in the numerical integration is given.

Differential Time Element: 0.05 seconds

Gravitational Acceleration: 32.2 ft/s<sup>2</sup>

Air Density: 0.00229 slug/ft<sup>3</sup>

Total Net Weight: 2.3 lbs

### **Wing**

Planform Area: 3.24 ft<sup>2</sup>

Aspect Ratio: 7.716

Oswald Efficiency Factor: 0.85

Angle of Zero Lift: -0.0515 rad (-2.9507°)

Lift Curve Slope: 4.007 rad<sup>-1</sup> (0.0699 deg<sup>-1</sup>)

### **Canard**

Planform Area: 1.388 ft<sup>2</sup>

Aspect Ratio: 5.552

Oswald Efficiency Factor: 0.85

**Angle of Zero Lift:** -0.0515 rad (-2.9507°)

**Lift-Curve Slope:** 3.755 rad<sup>-1</sup> (0.0655 deg<sup>-1</sup>)

**Propeller Thrust:** 0.25 lbs

**Constant Climb Angle-of-Attack:** 5°

Regarding the data just presented and the numerical integration technique in general, several items should be noted. First, the lift-curve slopes have already been corrected to account for the finite nature of the wing & canard, and it is this corrected value which is listed above and used by the computer routine.

Secondly, due primarily to the fact that there was not enough time available to experimentally measure the exact relationship between propeller thrust and airspeed for our particular propulsion package, it has been assumed that the propeller will be providing a constant thrust throughout the climb. Obviously, this is not true since a propeller's thrust is indeed a function of the advance ratio (which changes with the plane's airspeed). However, since the thrust provides a beneficial contribution to the climb, the error introduced by assuming that the thrust is constant can be minimized by choosing a slightly conservative value. For example, at a cruise speed of 25 ft/s the propulsion package should provide about 5 lbs of thrust, which is two times greater than the value used in the computer routine.

Furthermore, in order to effectively model the climbing motion of the airplane and determine the forces induced on it, it is necessary to make some sort of assumption concerning the angle-of-attack. Based primarily upon ease of calculations rather than actual experience, it has been assumed that the airplane will climb in such a manner that the wing & canard will always see the same effective attack angle. Because the relative wind will obviously change direction as soon as the airplane begins moving upward and will continue to change as the plane eventually loses energy (and hence velocity), this assumption would require the pilot to continually adjust the airplane's attitude during the entire ascent. Keeping the airplane at an exact angle-of-attack would undoubtedly be quite a difficult task. Nevertheless, it is an assumption which must be made in order model the climbing motion, and it seems to be a fairly

good approximation when averaged over the entire ascent phase. In an effort to minimize the error, a rather modest climb angle of  $5^\circ$  was chosen.

Finally, ground effect has not been included in the calculations. This was done in an attempt to balance out any unforeseen negative factors or errors not accounted for by the numerical integration method used.

### B.3 Zoom Take-off Computer Analysis Code

```

REM                                UNIVERSITY OF NOTRE DAME
REM                                DEPARTMENT OF AEROSPACE & MECHANICAL ENGINEERING
REM
REM                                AE441: AEROSPACE DESIGN
REM                                SPRING 1990
REM
REM                                GROUP E
REM                                ZOOM TAKE-OFF PERFORMANCE
REM
REM
REM VARIABLES USED:
REM
REM AOATTACK:    relative angle of attack seen by airfoils (radians)
REM AOLc:       angle of zero lift of canard (radians)
REM AOLw:       angle of zero lift of wing (radians)
REM ARc:        aspect ratio of canard
REM ARw:        aspect ratio of wing
REM BETA:       'downwash' angle due to vertical velocity (radians)
REM CDOc:       zero-lift drag coefficient of canard
REM CDOW:       zero-lift drag coefficient of wing
REM CLc:        lift coefficient of canard
REM CLw:        lift coefficient of wing
REM D:          net drag (lbf)
REM DT:         differential time element (seconds)
REM DVX:        differential horizontal speed (feet/second)
REM DVY:        differential vertical speed (feet/second)
REM DX:         differential horizontal distance (feet)
REM DY:         differential vertical distance (feet)
REM Ec:        Oswald efficiency factor of canard
REM Ew:        Oswald efficiency factor of wing
REM G:          gravitational acceleration (feet/second^2)
REM INCLIN:    inclination of airplane relative to horizontal (radians)
REM L:          net lift (lbf)
REM LCSc:      lift-curve slope of canard (radians^-1)
REM LCSw:      lift-curve slope of wing (radians^-1)
REM RHO:       air density (slug/feet^3)
REM Sc:        surface area of canard (feet^2)
REM Sw:        surface area of wing (feet^2)

```

REM T: propeller thrust (lbf)  
 REM TOTAL TIME: net time from point of take-off (seconds)  
 REM V: net velocity seen by airfoils (feet/second)  
 REM VNX: "new" horizontal speed (feet/second)  
 REM VNY: "new" vertical speed (feet/second)  
 REM VOX: "old" horizontal velocity (feet/second)  
 REM VOY: "old" vertical velocity (feet/second)  
 REM W: net weight (lbf)  
 REM X: horizontal position relative to take-off point (feet)  
 REM Y: vertical position relative to take-off point (feet)

PI=4\*ATN(1)

DT=.05

TOTALTIME=0

VOX=40

VOY=0

X=0

Y=0

W=2.3

G=32.2

RHO=.00229

CDO = .04

Sw=3.24

ARw=7.716

Ew=.85

AOLw=-.0515

LCSw=4.007

Sc=1.388

ARc=5.552

Ec=.85

AOLc=-.0515

LCSc=3.755

T=.25

AOATTACK=.0873

REPEAT:

BETA=ATN(VOY/VOX)

INCLIN=AOATTACK+BETA

CLw=LCSw\*(AOATTACK-AOLw)

CLc=LCSc\*(AOATTACK-AOLc)

V=(VOX^2+VOY^2)^.5

Lw=.5\*RHO\*V^2\*(Sw\*CLw)

Lc=.5\*RHO\*V^2\*(Sc\*CLc)

L=Lw+Lc

D=.5\*RHO\*V^2\*Sw\*(CDO+CLw^2/PI/Ew/ARw)+.5\*RHO\*V^2\*Sc\*(CLc^2/PI/Ec/ARc)

```
DVX=G/W*(T*COS(INCLIN)-D*COS(BETA)-L*SIN(BETA))*DT
DVY=G/W*(T*SIN(INCLIN)-D*SIN(BETA)+L*COS(BETA)-W)*DT
```

```
VNX=VOX+DVX
VNY=VOY+DVY
```

```
DX=(VOX+VNX)/2*DT
DY=(VOY+VNY)/2*DT
```

```
X=X+DX
Y=Y+DY
VOX=VNX
VOY=VNY
```

```
TOTALTIME=TOTALTIME+DT
```

```
CUTOUT:
```

```
CLS
PRINT "TOSPEED: ";TOSPEED;
PRINT " NET TIME: ";TOTALTIME;" SECONDS"
PRINT " HORIZONTAL POSITION: ";X;" FEET"
PRINT " VERTICAL POSITION: ";Y;" FEET"
PRINT " HORIZONTAL SPEED: ";VNX;" FEET/SECOND"
PRINT " VERTICAL SPEED: ";VNY;" FEET/SECOND"
PRINT " INCLINATION OF PLANE: ";INCLIN*180/PI;" DEGREES"
PRINT " ANGLE OF ATTACK: ";AOATTACK*180/PI;" DEGREES"
PRINT " LIFT FORCE OF WING: ";Lw
PRINT " LIFT FORCE OF CANARD: ";Lc
PRINT
IF V<25 THEN PRINT "DANGER . . . STALL WARNING"
```

```
GET A$
IF A$="Q" OR A$="q" THEN STOP
GOTO REPEAT:
```

```
END
```

#### **B.4 Validation of Numerical (Computer-Derived) Results**

As a rough validation of the numerical integration technique performed by the microcomputer routine given in section B.3, assume that no forces other than gravity are exerted on the plane after liftoff. If this were the case, then the kinetic energy at take-off must equal the potential energy gained plus the remaining kinetic energy at altitude.

i.e. For Weight: 2.4 lbs

Take-off Speed: 40 ft/s



Speed at Altitude: 25 ft/s (cruise speed)

$$\text{K.E.}_1 + \text{P.E.}_1 = \text{K.E.}_2 + \text{P.E.}_2$$

$$(1/2)mV_1^2 + 0 = (1/2)mV_2^2 + mgh$$

$$(1/2)V_1^2 = (1/2)V_2^2 + gh$$

$$(1/2)(40 \text{ ft/s})^2 = (1/2)(25 \text{ ft/s})^2 + (32.2 \text{ ft/s}^2)h$$

Therefore,  $h = 15.1$  feet.

Confirmed by the computer-derived results presented in Figure 7.2, this height is quite close to that predicted by the numerical integration method (16.5 feet). (NOTE: After take-off there are definite forces exerted on the airplane besides gravity. Therefore, the validation method outlined above can only provide a general check as to whether a more sophisticated method seems to be giving plausible results, which it does.)